

1. Study on Performance Improvement of  
GaN-based Light Emitting Diodes Grown on  
Silicon (111) Substrate



# **Study on Performance Improvement of GaN-based Light Emitting Diodes Grown on Silicon (111) Substrate**

## ***Abstract***

Commercially available GaN-based optoelectronic devices, such as light-emitting diodes (LEDs), have been grown on sapphire or SiC substrates since the last century. Comparing with these substrates, silicon (Si) substrate is attractive for GaN-based devices because of many merits, such as low cost, good thermal conductivity and integration potential in the device fabrication. However, it is still a challenging issue to grow device-quality GaN epitaxial layers on Si due to the large mismatch in lattice constants and thermal expansion coefficients. Recently, considerable efforts have been focused on the growth of high quality GaN on Si.

In this report, two approaches to improve the performance of GaN-based LEDs grown on Si (111) have been presented. Some corresponding measurements have been performed to characterize structure property and device performance, such as AFM, XRD, TEM, EL, and  $I-L-V$ . One is demonstration by using an intermediate layer of 3C-SiC. As a result, the device with 3C- SiC IL showed an enhanced light output power by a factor of 2.4 at a drive current of 20 mA. The superior device performance was attributed to the improvement in the structural properties. Another one is changing the thickness of n-GaN to improve the performance of LEDs. As one consequently, the 1.7 mW output power of LEDs with a high saturation operating current of 280 mA have been realized. In addition, as the n-GaN thickness increases from 1 to 2  $\mu\text{m}$ , the light output powers of the LEDs have enhanced approximately two times under the injection current of 20 mA. Moreover, the maximum values of respective external quantum efficiency are achieved as 0.3 and 0.6%, respectively. Therefore, this study implies that both of the two approaches are the effective methods for enhancing the light output power of LEDs grown on Si substrate.

# **1. Introduction**

## **1.1 Background of this study**

In the last century, many progress in silicon fabrication technology has been created to information society in industry. These progress in information technology industry further has been demanded for immediate and low-latency access for a large volume of date, which then has merged into information and communication technology (ICT). Worldwide spreading of internet is the core factor, which has already pushed rapid development in the industry. Moreover, since the early 21st century, a new ubiquitous society has started to be born through the advancement in ICT industry. In ubiquitous society, access to information is anytime, anywhere, with anyone and with anything [1].

As a result for information accessibility in this society, copper-based cable communication can no longer serve the large volume of information at low-latency, which then pushed for optical-based communication like fiber-optics. Cell phone previously a medium for voice communication has emerged into smart phone, which can carry voice, video, and date communications, demanding for more base stations with more efficient use of wavelength to serve the growing volume of date transmission. Radio and video broadcast through analog wave signal need to be converted into digital signal to significantly improve radio wave utilization, while at the same time broadcasting more imformation with better quality to the audiences. Vehicles previously a solely mechanical products with combustion engine, have emerged into smart vehicles with mechanical-electrical hybrid engine, supported by intelligent transportation system for improved safety, security and efficiency in surface transportation system.ubiquitous

society has demanded for enormous utilization of resources and electricity. The vast amounts of date also need to be efficiently stored and archived, which demanded for higher density date storage [1].

Fortunately for the material system, III-nitride-based materials can be applied in wide area of optoelectronics and electronics products. As shown in Fig. 1.1, the wide bandgap energy of III-nitride alloys from 0.7 eV for InN to 6.2 eV for AlN can cover the whole light spectrum from deep ultra-violet until IR regin.

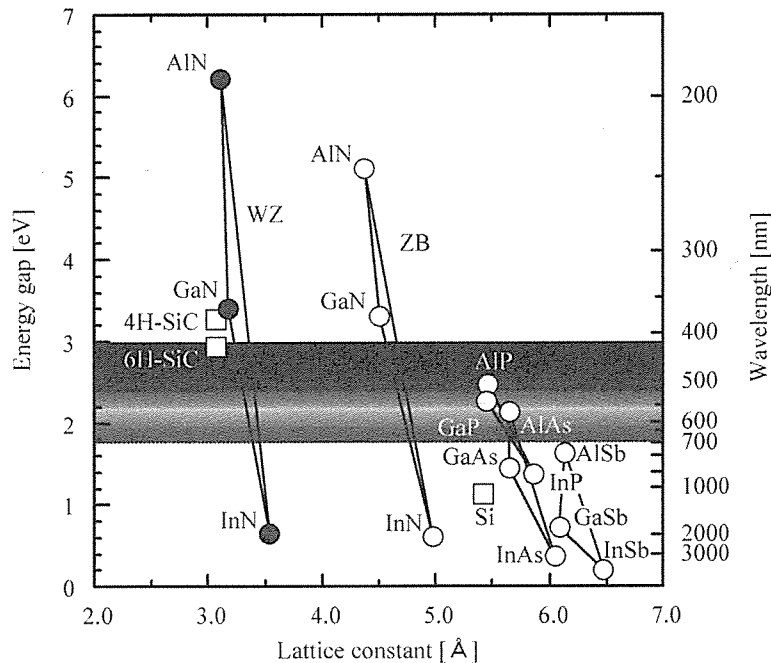


Fig. 1.1. Band-gap energy as a function of lattice constant for common semiconductor materials including III-nitride alloys.

Nowaday, the new history will be written in the 21 century. During the course of society developing, human will be confused when meeting some more serious problems, such as water, food, environment and so on. It is believed that the most important problem should be limitation of resource, especially, regarding energy problem, the corresponding measures must be immediately taken into accounted in the future. The world-wide photo, which was taken from satellite in the sky for the

electrical light in the night, is shown in the Fig. 1.2. Based on this figure, comparing the different area, it is obvious that energy consumption is losing its balance because of technology and economy gap. Nevertheless, the responsibility of saving engery will become to be more and more significant in the following years. Consequently, it can be expected that the development of wide band-gap nitride-based material research would give its contribution for solving or relieving these scoiety problems.

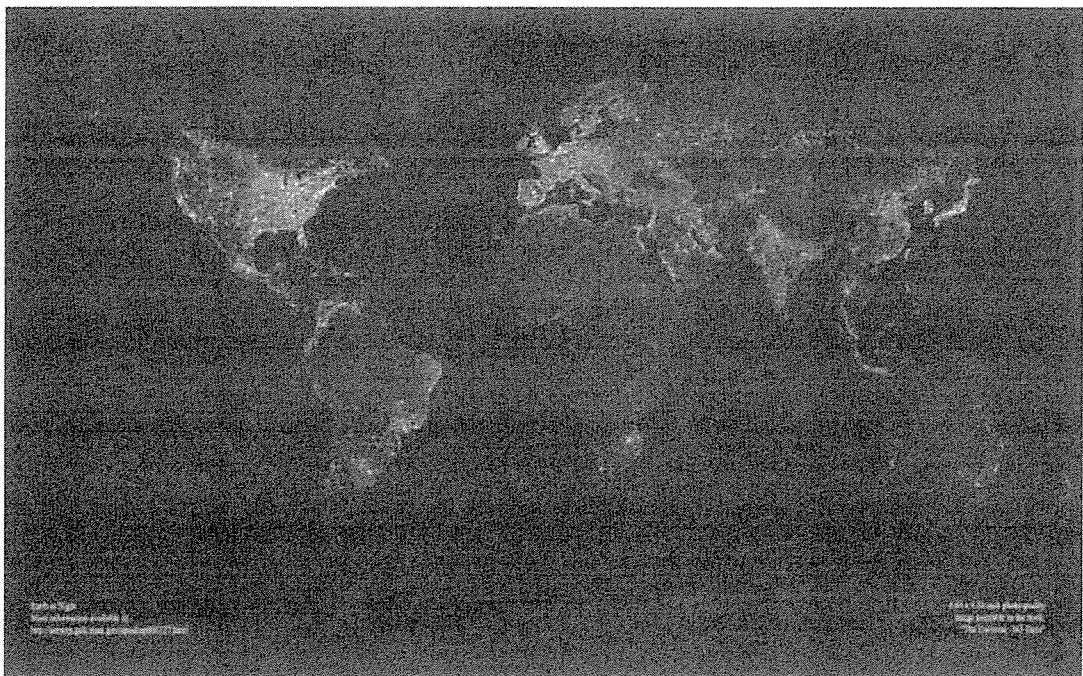


Fig. 1.2.The world-wide satellite photo of electrical light in the night [2].

Actually, gallium nitride technology was once deemed too expensive to replace silicon technology. However, if some successes can be made in the growing high qulity GaN on a silicon wafer, which would make the technology more economical. In terms of the Si substrate, the substrate costs around fifty cents per square centimetre, which is much cheaper than the usual substrates, such as sapphire or SiC, which cost about five dollars, or even twenty dollars/cm<sup>2</sup> in the case of SiC. Moreover, using silicon, large wafers measuring thirty centimetres in diameter can be produced, which is not possible with sapphire and SiC.

However, because GaN and silicon have different material properties, it is difficult to combine the two materials on a wafer, cracks may form during heating, for instance, as the materials expand to a different degree. Recently, lots of research group, including our group, have found ways to grow high quality GaN on silicon and solved around this problem. As aforementioned, most transistors in the world are still based on silicon. This semiconductor does not just serve as a substrate, but also the base material of transistors and chips. That is, pretty much everything in electronics is still made of silicon. It's a fabulous material. Unfortunately, silicon also has its drawbacks. At high temperatures above 200°C silicon-based components begin to malfunction. On the other hand, the present popular and active research target, that is, GaN transistors, can withstand temperatures of up to 1000°C, which makes the material attractive for building sensors in car engines.

Moreover, GaN can withstand electrical fields that are up to fifteen times stronger than in silicon, the electrons also move more quickly in GaN than in silicon, which enables faster circuitry. In fact, this is especially important for telecommunications since the information is processed more rapidly and efficiently. Thanks to its heat resistance, power electronics made of GaN barely requires cooling. If the base stations of mobile communications installations were equipped with GaN transistors, for instance, the providers would not need power-guzzling cooling systems. In addition, conventional base stations require ten kilowatts input to emit just one kilowatt. Therefore, a lot of energy is thus wasted, which ultimately costs the environment and consumers dearly. If silicon electronics were to be replaced with GaN-Si electronics, a lot of energy could be saved. As well known, gallium nitride is therefore just the ticket for use in many areas of electronics, especially power

electronics. Herein, it should be noted that GaN can help to save energy in lighting, which is currently responsible for a fifth of the global electricity consumption. A five-watt LED lamp based on GaN, however, generates the same amount of light as a conventional sixty-watt bulb, which makes enormous energy savings possible. The same also goes for voltage conversion in appliances. When plugging a PC into a 230-volt socket, a converter inside the appliance provides the right voltage to the chips, such converters can be more efficient with GaN technology. Experts have already estimated that the global energy consumption could be reduced by a quarter if the energy were used intelligently at the place of consumption. One of the most important things is, that GaN transistors have shown to be lightning-fast and allow frequencies of up to 205 gigahertz, it is more than enough to make computers, mobile phones, and power electronics quicker, smaller and more economical [3].

General speaking, everything is there to help this technology make a breakthrough. What's lacking is an industrial partner that wants to launch gallium nitride silicon electronics on the market. At the same time, just why telecommunications companies did not already convert to GaN technology, the answer is very clear, because the conversion costs a huge sum of money. In the ideal scenario, silicon components could be replaced with GaN power electronics when required. Consequently, it can be imagined that support for the changeover will come from the political arena: introducing a strict CO<sub>2</sub> emission guidelines, for instance, would encourage companies to reduce their energy costs. This would incite telecommunications companies for example to invest in greener technologies and to reduce CO<sub>2</sub> emissions. Also, people can look forward to realizing the almost ultimate dream some day.

## **1.2 Development of wide band-gap nitride-based light emitting diodes**

As well known, stupendous progress has been made in development of the III-nitride AlN, GaN, InN, and their family of material alloys for optoelectronics and electronics applications since last century [4-5]. Wurtite InN, GaN, and AlN have direct room-temperature bandgaps of 0.7 eV, 3.4 eV, and 6.2 eV respectively [6]. The entire spectral region, from infrared to ultraviolet, can be covered, which is impossible with the other III-V materials system, such as gallium Arsenic (GaAs)-based and phosphide (P)-based alloys. It makes the nitride system be attractive for optoelectric device applications, such as light-emitting diodes (LED), laser diodes (LD), and detectors, in particular, the combination of GaN-based blue and green LEDs with GaAs-based red LEDs forms for full-color displays and solid-state white light illumination. At present, incandescent bulbs and fluorescent lamps are used as light sources and many applications, which have poor reliability, durability, and a low luminous efficiency. By using a solid-state white light source to replace the conventional incandescent bulbs or fluorescent lamps would provide not only a longer life time, but also reduce the power consumption. Also, III-nitride materials are promising for high temperature/high power/high breakdown field applications.

On the other hand, the first electroluminescence from GaN was announced at the Radio Corporation of America (RCA) in the summer of 1971 by Jacques Pankove et al. At that time, the sample consisted of an insulating Zn-doped layer which was contacted with two surface probes, and blue light centered at 475 nm was emitted [7] as presented in Fig. 1.3. Then, they made a device consisting of a metal-insulator-semiconductor (MIS) diode. This was the first current-injection GaN light emitter [8]. In April 1972, the RCA team (Paul Maruska et al.) decided that magnesium (Mg) might

be a better choice of p-type dopant than zinc. They began growing Mg-doped GaN films using the Halide Vapor Phase Epitaxy (HVPE) technique, and on July 7, 1972, got a blue and violet emission at 430 nm [9]. These devices were inefficient due to lack of p-type conductivity, even though they were Mg doped, the luminescence in these films was probably mediated by minority carrier injection or impact ionization in the high-field insulating region of the films. Unfortunately, at the beginning of 1974, the RCA Corporation was collapsing as revenues plunged. Therefore, the corresponding blue LED project was cancelled. In the years subsequent to the collapse of RCA, work on GaN virtually ceased everywhere, and in 1982 only a handful of papers were published world-wide on this material.

**The first electroluminescence from GaN**

(J. I. Pankove et al., J. Luminescence 4, 63, 1971)

**The first current-injection GaN light emitter**

(J. I. Pankove et al., RCA Review 32, 383, 1971)

**Mg for GaN p-type doping**

(H. P. Maruske et al., Mat Res. Bull. 7, 777, 1972)

**The first true GaN p-type doping**

(H. Amano et al., Jpn. J. Appl. Phys. 28, L2112, 1989)

**The first GaN p-n-homojunction LED**

(I. Akasaki et al., Inst. Phys. Conf. Sur. 129, 851, 1992)

**Blue and green GaN LEDs with EQE of over 10%**

(S. Nakamura et al., Jpn. J. Appl. Phys. 34, L797, 1995)

**The first viable blue laser CW operating at RT**

(S. Nakamura et al., Appl. Phys. Lett. 69, 4056, 1996)

1970

1980

1990

2000

Fig. 1.3. Evolution of III-nitride-based semiconductor.

However, Isamu Akasaki and co-workers Amano et al. in Nagoya of Japan

didn't want to give up. They succeeded in growing the first high quality GaN single crystal in the world by using the LT-AlN buffer layer in 1985 [10], and finally in 1989, they continued to demonstrate the first true p-type doping, with achieving conducting material with electron-beam annealed Mg-doped GaN [11]. In 1992, the first GaN p-n-homojunction LED was reported by Akasaki et al [12]. The efficiency of the LED is approximately 1%, which is not affected by dislocations in the same adverse manner as III-V As-based and P-based light emitters. In 1992, p-type GaN was also produced by thermal annealing of Mg-doped GaN grown with the LT-GaN buffer layer by Nakamura et al. at Nichia Chemical Industries [13]. In 1995 they developed blue and green GaN hetero-structure LEDs with the efficiencies of exceeding 10% [14] and demonstrated the first viable blue laser pulse and CW operating at room temperature in 1996 [15]. With these technique developments and achievements, much progress is expected in the area of solid-state lighting. The history of improvement in the efficiency for light emitting diodes is shown in Fig. 1.4, from which the trend of LEDs can also be judged.

And, some data about the incandescent and fluorescent lamp are also presented.

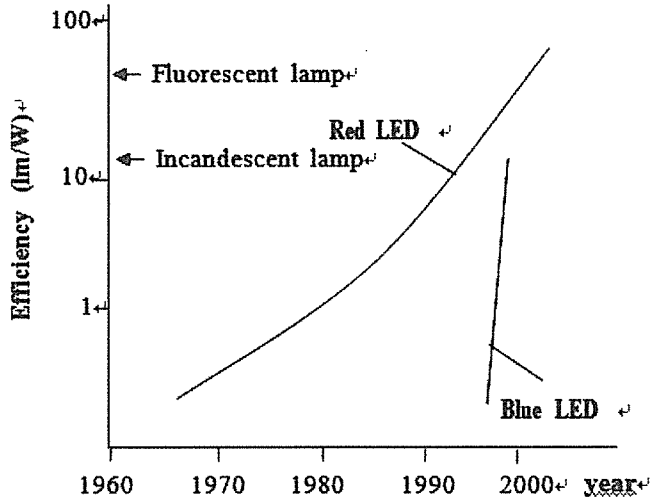


Fig. 1.4. The history of improvement in the efficiency for LED.

## References

- [1] B. A. B. Ahmad Shuhaimi, *Research on Improvement of GaN-based Light Emitting Devices Grown on Silicon (111) Substrate*. Ph. D. Thesis, ch.1 March, (2010).
- [2] R. E. Smalley, Energy & Nano Technology, Conference, Rice University. May. 3, (2003).
- [3] Compound Semiconductor, “GaN-on-silicon transistors are faster and smaller”, Sept. 27, (2011).
- [4] S. Nakamura, and S. F. Chichibu, *Introduction to Nitride Semiconductor Blue Lasers and Light Emitting Diodes*. London: Taylor & Francis, ch.1(2000).
- [5] S. J. Peraton, C. R. Abernathy, and F. Ren, *Gallium Nitride Processing for Electronics, Sensors and Spintronics*. London: Springer-Verlag, ch. 3 (2006).
- [6] H. Morkoc, *Handbook of Nitride Semiconductors and Devices*. Weinheim: Wiley-VCH, , ch. 1(2008).
- [7] J. I. Pankove, E. A. Miller, D. Richman, and J. E. Berkeyheiser, J. Lumin. **4**, 63 (1971).
- [8] J. I. Pankove, E. A. Miller, D. Richman, and J. E. Berkeyheiser, RCA Review, **32**, 383( 1971).
- [9] H. P. Maruska, W. C. Rhines, and D. A. Stevenson, Mat. Res. Bull. **7**, 777 (1972).
- [10] H. Amano, N. Sawaki, I. Akasaki, and T. Toyoda, Appl. Phys. Lett. **48**, 353 (1986).

- [11] H. Amano, M.Kito, K. Hiramatsu, and I. Akasaki, Jpn. J. Appl. Phys. **28**, L2112 (1989).
- [12] I. Akasaki, H. Amano, K. Itoh, N, Koide, and K. Manabe, GaAs and Related Compounds conference, Inst. Phys. Conf. Ser.,**129**, 851 (1992).
- [13] S. Nakamura, T. Mukai, M. Senoh and N. Iwasa, Jpn. J. Appl. Phys. **31**, L139 (1992).
- [14] S. Nakamura, M. Senoh, N. Iwasa, and S. Nagahama, Jpn. J. Appl. Phys. **34**, L797 (1995).
- [15] S. Nakamura, M. Senoh, S. Nagahama, N. Iwasa, T. Yamada, T. Matsushita, Y. Sugimoto, and H. Kiyoku, Appl. Phys. Lett. **69**, 4056 (1996).

## **2. III-nitride epitaxial growth by MOCVD**

### **2.1 Introduction**

Nowaday, it is believed that one of the hottest research areas is in the GaN-based material system , which has always been actively studied because of many applications in high-performance device, such as high-density optical data storage, light emitting diodes for illumination and power electronics. However, the biggest hindrence in the early starting years of GaN-based epitaxy growth is no natural GaN substrate, which has incited researchers to depend on epitaxial growth using different substrate materials, that is called to hetero-epitaxy. Therefore, the corresponding substrate, at least, whose constants in the lattice and thermal expansion coefficient should be nearly matched to the ones of GaN. Normally, Si, sapphire, SiC, and GaN substrates have been employed in the research.

### **2.2 Substrate comparison for GaN epitaxial growth**

GaN-based materials have been usually grown on sapphire substrate due to its considerably good properties and variable applications. However, sapphire has a few limitations, such as its native physical property as an insulator, it prevents fabrication of device with vertical-type electrode structure. Also, sapphire has a relatively low thermal conductivity, which restricts thermal dissipation in high-power devices. On the other hand, maximum diameter size for sapphire wafer is limited to 4 inches, it will hinder commercial mass production of GaN.

Hetero-epitaxy of GaN on 6H-SiC has been tremendously investigated by several groups [5,6], with the successful fabrication of electronic and optoelectronic devices, such as high electron mobility transistor (HEMT) [7], light emitting diode

(LED) [8], and laser diode (LD) [9,10]. However, 6H-SiC substrate has limited availability, restricted to small diameter size and relatively far more expensive than sapphire and silicon substrate, which limits mass production quantity and interests for device fabrication.

As well known, homo-epitaxy of GaN on free-standing GaN substrate has reached dislocation density as low as  $10^6 \text{ cm}^{-2}$  [11]. In addition, such substrate has maximum diameter size of only 2 inches and very limited availability, which leads to its price to become extremely expensive. Therefore, it is only employed in high-performance devices, for which the corresponding low dislocation density is significant necessary such as blue-violet LD.

While epitaxy growth technology of GaN on sapphire, 6H-SiC and GaN free-standing substrate can be already considered well established, there are lots of demands for the other breakthrough for GaN-based epitaxy on silicon (Si) substrate. Regarding the Si substrate, there are many charming points, for instance, excellent availability, large diameter size of up to 12 inches, and very low cost. The best advantage in successful growth of GaN-based devices with well-established Si-based electronic device, for example, integrated-circuits, photo-detector, and so on, allowing fabrication of multi-fuction hybrid device on a single wafer.

Comparing with sapphire substrate, Si is a native semiconductor, its electrical conductivity can be controlled by doping, allowing the fabrication of devices with vertical-type electrode structure. Si has better thermal conductivity than sapphire, which improves thermal dissipation, in particular, for high-temperature device operation. Some parameters can be referred in the Table II-I.

Table II-I: Comparison of substrate for GaN epitaxial growth [1-4].

		GaN	AlN	Si(111)	6H-SiC	sapphire
lattice constant	a	(Å)	3.189	3.11	5.43	3.08
	c	(Å)	5.185	4.98	-	12.991
thermal conductivity		(W./cmK)	1.3	2.85	1~1.5	3.0~3.8
thermal expansion	in-plane	( $\times 10^6$ /K)	5.59	4.2	2.59	4.2
lattice mismatch GaN/substrate		(%)	-	2.4	-16.9	3.5
thermal mismatch GaN/substrate		(%)	-	33	116	33
					-25	

However, GaN epitaxy on Si substrate is more challenging than that of on sapphire or SiC substrates. Large thermal coefficient mismatch of 116% between the GaN and Si is thought as the main reason for cracks(as shown in Fig. 2.2-b) to occur during cooling down after growth, even though lattice constant mismatch for GaN/Si(111) of -17% is almost similar to GaN/sapphire of 16% as shown in Fig. 2.1. At the same time, the mechanism of strain happening is shown in the Fig. 2.1. On the other hand, GaN-Si reaction during growth causes amorphous meltback-etching layer (Fig. 2.2-c) when using conventional growth technology (Fig. 2.2-a). Then, Si gas from the substrate caused low-doping density in p-type GaN epitaxial layer. These growth challenges have been presented by many approaches of buffer layer techniques to obtain high quality GaN epitaxy on Si substrate.

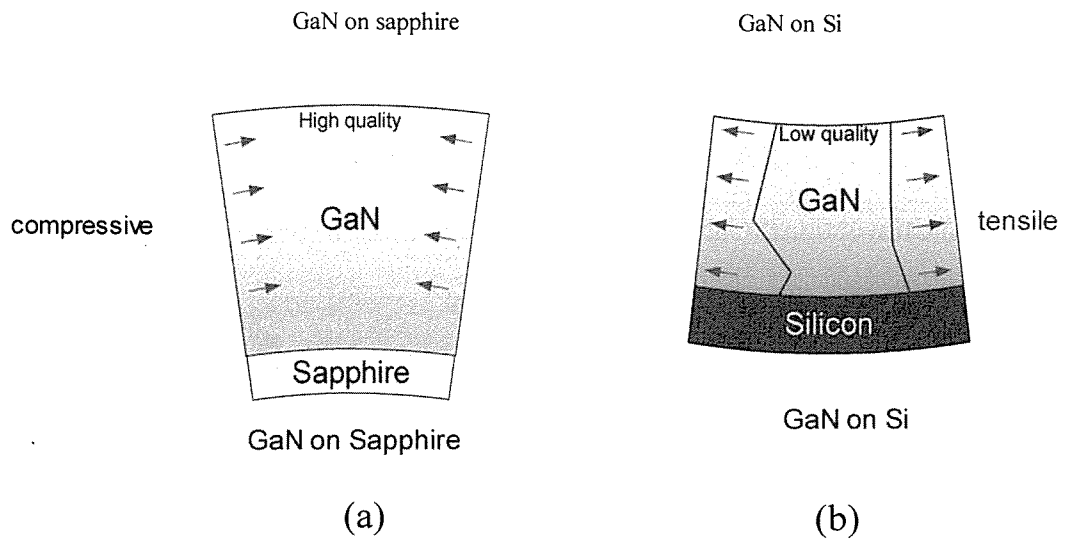
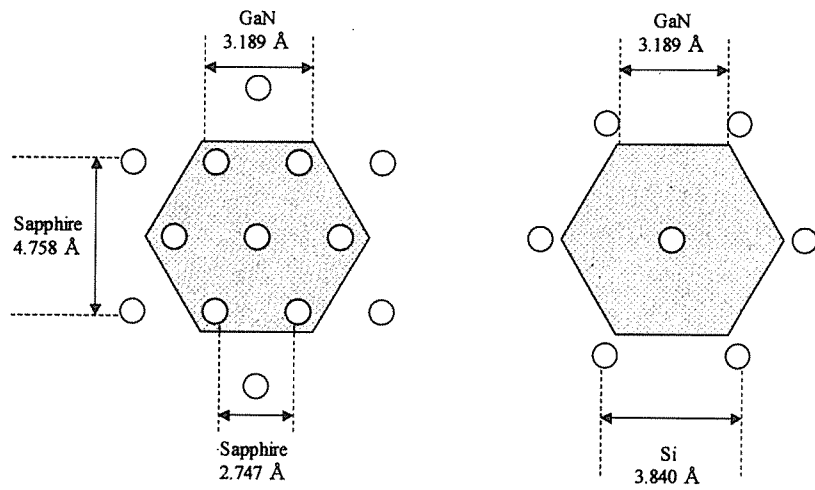


Fig. 2.1. Mechanism of lattice mismatch and strain happening in GaN grown on (a) sapphire substrate and (b) Si (111) substrate.

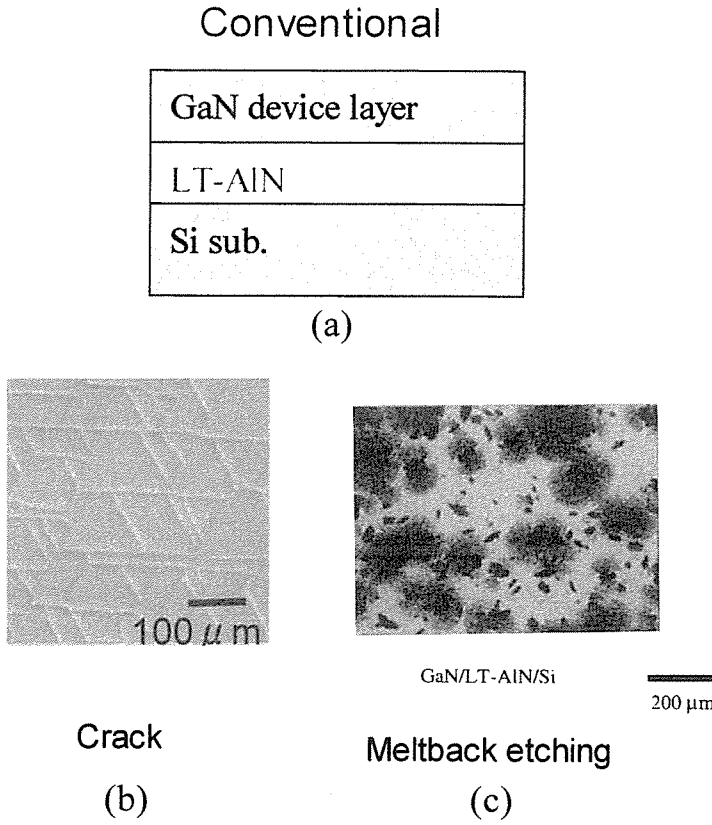


Fig. 2.2. (a) Conventional GaN epitaxial growth method, (b) Some cracks have occurred on the surface, and (c) image of meltback etching.

GaN epitaxy on Si substrate has typical dislocation density of around  $10^9\text{-}10^{11}$   $\text{cm}^{-2}$  [12], and can still be improved by optimizing its growth techniques. However, as shown in Fig. 2.2, GaN grown on Si with low-temperature AlN layer is more prone to cracks when the growth temperature is cooled down to room temperature (RT), which results from the large thermal expansion difference and lattice mismatch. In the case of sapphire substrate, GaN epilayer undergoes compressive strain when growth temperature is returned to RT. In contrast, GaN epilayer grown on Si substrate suffers tensile stress when growth temperature is cooled down to RT making Si substrate more prone to cracks comparing with sapphire substrate, especially, when the GaN thickness is over 1  $\mu\text{m}$ .

This research concentrates on GaN epitaxy on Si substrate grown with high-temperature AlN nucleation layer and AlN/GaN strained-layer superlattice (SLS). Further improvement on material and optical properties have been realized by using the template of 3C-SiC/Si(111) and increasing the n-GaN thickness to 2  $\mu\text{m}$ .

## 2.3 GaN epitaxial technique grown on Si substrate

Buffer and intermediate layers have been extensively investigated by many research groups for GaN growth on Si substrate, such as Al/AlGaN buffer and AlN/GaN SLS [13-16], AlN interlayer [17] and  $\text{Si}_x\text{N}_{1-x}$  interlayer [18]. This research focuses on crystalline quality improvement for GaN epitaxy on Si substrate by using the template of 3C-SiC/Si(111) and increasing the n-GaN thickness to 2  $\mu\text{m}$ . Variable buffer and/or intermediate layer growth techniques as aforementioned above, including epitaxial lateral overgrowth (ELO) [19] and pendo epitaxial overgrowth (PEO) [20], are not discussed in this dissertation.

### 2.3.1 AlN/AlGaN buffer layer

AlN/AlGaN layer is used to prevent formation of meltback-etching when GaN epilayer is grown on Si substrate. It also acts as intermediate layer to create a high density nucleation growth. In the growth of sapphire substrate, high density nucleation growth is achieved by low-temperature GaN buffer layer. However, in the case of growth on Si substrate, low-temperature GaN buffer can not be used because of GaN-Si reaction, which has been already explained in the above section. Therefore, materials such as AlN and AlGaN, which are stable at high temperature are preferred for high density nucleation growth. Usage of AlN layer as nucleation layer for GaN growth on Si

substrate has been reported by many group [21-26]. While, this approach suffers poor surface flatness, it influences the subsequent layer growth. It is presented that 170 nm GaN layer has grown on the initial AlN nucleation layer [27], In addition, it depends on the Al composition, AlGaN has relatively better coating property and it easier to grow [28]. Consequently, AlGaN is considered as one of good candidates for intermediate layer. Our research group has presented AlN/AlGaN buffer layer to take advantage of the combined material properties [13-16]. That is, AlN layer which is stable at high-temperature is initially grown on Si substrate to create a high density nucleation layer, followed by AlGaN layer to obtain a layer with good smooth surface.

### **2.3.2 AlN/GaN strained-layer superlattice (SLS)**

Multilayer and/or strained-layer superlattice (SLS) growth technology is significant to control crack generation in III-nitride-based semiconductor layer growth. In III-nitride layer growth on Si substrate, reactor temperature ramp-down to RT generates concave wafer curvature, and cracks on the epitaxial layer due to the difference of thermal expansion coefficient between III-nitride epitaxial layer and Si substrate, leading to the difficulty of thick GaN epitaxial layer, Thus, optimization in the epitaxial structure is necessary to successfully grow high quality crack-free thick GaN-based layer on Si substrate. The importance of growing thick epitaxial GaN layer can be expressed in the device structure, it is fortunate that improving the material quality can be realized as using AlN/GaN SLS in controlling wafer curvature and cracks. SLS is also effective to reduce misfit dislocations resulted from lattice mismatch of GaN-based epitaxial layer and the underlying Si substrate. Threading dislocation (TDs) can be modulated to prevent them from penetrating to the surface using SLS, an

approach which has already been used previously in GaAs-based growth on Si substrate [27,29-30]. When a stack of two types of material with different lattice constant is grown coherently, lattice strain is built upon the interface of the two different materials giving a strong strain when they are accumulated together. Therefore, TDs which reach the interface are bent by the strain, and reaction between inclined TDs will create dislocation close-loop, eliminating the TDs from penetrating vertically into the epitaxial surface. The SLS structure creates multiple bulit-up interface strain for TDs inclination, thus, it is possible to control penetrations of TDs into the subsequent epitaxial layers. If the lattice strain is weak, it is not possible to bend the treading dislocations causing it to penetrate through the SLS. Moreover, if the lattice strain is too large, new misfit dislocation might be built due to the strain. In this research, a SLS consisting of periodes of AlN and GaN stacks with respective layer thickness optimized values of 5 and 20 nm is employed as the fundamental intermediate layer, followed by further optimization in the succeeding layer.

## 2.4 MOCVD equipment in this study

In this reseach, a commercial MOCVD reactor system (Nippon Sanso SR-4000) has been used for the epitaxial growth of InGaN-based multiple-quantum wells (MQWs) LEDs structure. The photo of outward appearance is shown in Fig. 2.3. At the same time, Figure 2.4 shows the design schematics of the corrossponding MOCVD reactor. Herein, it should be noted that epitaxial growth in our system can be used for one 4-inch or three 2-inch wafer. Also, the growth pressure can be easily controlled automatically in the range from low (100-300 torr) to normal air pressure (760 torr).

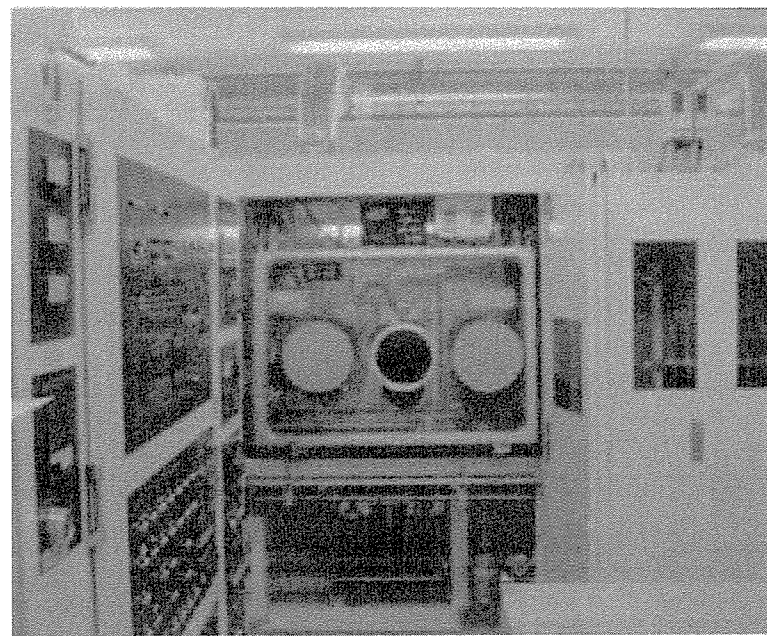


Fig. 2.3. The appearance of Nippon Sanso SR-4000 MOCVD system.

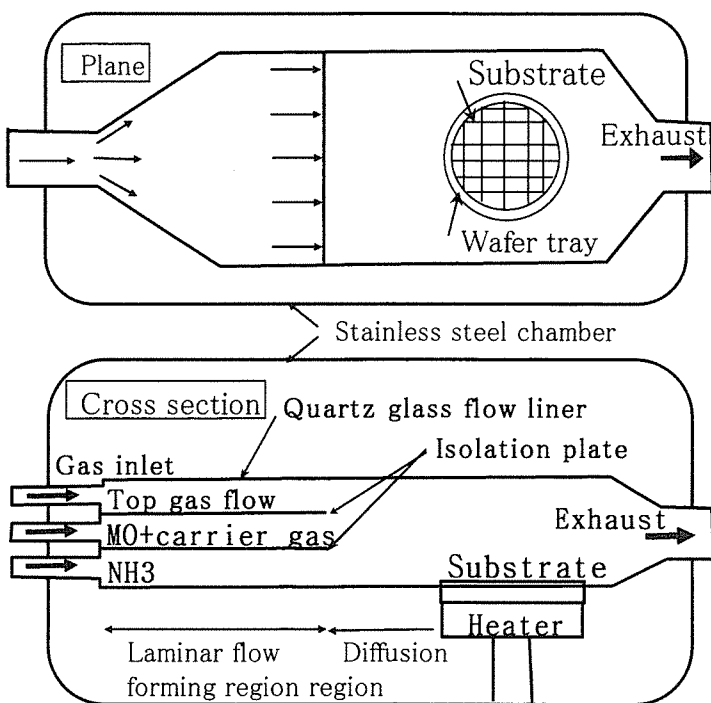


Fig. 2.4. The design schematics of the above MOCVD reactor.

## References

- [1] S. Nakamura, S. Pearton, and G. Fasol, *The Blue Laser Diode*, Springer-Verlag, Berlin, Germany (2000)
- [2] S. Nakamura, and S. F. Chichibu, *Introduction to Nitride Semiconductor Blue Lasers and Light Emitting Diodes*. Taylor & Francis, New York, USA (2000).
- [3] J. Piprek, *Nitride Semiconductor Devices Principles and Simulation*, Wiley-VCH Verlag, Weinheim, Germany (2007).
- [4] K. Takahashi, *Wide-Gap Semiconductor Optical and Electronic Device*, Morikita Publishing, Tokyo, Japan (2006).
- [5] M. A. L. Johnson, S. Fujita, W. H. Rowland, K. A. Bowers, W. C. Hughes, Y. W. He, N. A. El-Masry, J. W. Cook, J. F. Schetzina, J. Ren, and J. A. Edmond, *J. Vac. Sci. Technol. B* **14**, 2349 (1996).
- [6] J. T. Torvik, M. Leksono, J. I. Pankove, B. V. Zeghbroeck, H. M. Ng, and T. D. Moustakas, *Appl. Phys. Lett.* **72**, 1371 (1998).
- [7] J. Bernát, M. Wolter, A. Fox, M. Marso, J. Flynn, G. Brandes, and P. Kordoš, *Electron Lett.* **40**, 78 (2004).
- [8] H. S. Kong, M. Leonard, G. Bulman, G. Negley, and J. Edmond, *Mat. Res. Soc. Symp. Proc.* **395**, 903 (2005).
- [9] A. Kuramata, K. Hirino, and K. Domen, *Fujitsu Sci. Tech. J.* **34**, 191 (1998).
- [10] J. Edmond, A. Abare, M. Bergman, J. Bharathan, K. L. Bunker, D. Emerson, K. Haberern, J. Ibbetson, M. Leung, P. Russel, and D. Slater, *J.Cryst. Growth* **272**, 242 (2004).

- [11] S. Hashimoto, Y. Yoshizumi, T. Tanabe, and M. Kiyama, *J. Cryst. Growth* **298**, 871 (2006).
- [12] Y. B. Pan, Z. J. Yang, Z. T. Chen, Y. Lu, T. J. Yu, X. D. Hu, K. Xu, and G. Y. Zhang, *J. Cryst. Growth* **286**, 255 (2006).
- [13] T. Egawa, B. Zhang, N. Nishikawa, H. Ishikawa, T. Jimbo, and M. Umeno, *J. Appl. Phys.* **91**, 528 (2002).
- [14] H. Ishikawa, K. Asano, B. Zhang, T. Egawa, and T. Jimbo, *Phys. Stat. Sol. A* **201**, 2653 (2004).
- [15] T. Egawa, B. Zhang, and H. Ishikawa, *IEEE Elect. Dev. Lett.* **26**, 169 (2005).
- [16] B. Zhang, T. Egawa, H. Ishikawa, Y. Liu, and T. Jimbo, *Jpn. J. Appl. Phys.* **42**, L226 (2003).
- [17] A. Dadgar, *Jpn. J. Appl. Phys.* **39**, L1183 (2000).
- [18] T. Riemann, T. Hempel, J. Christen, P. Veit, R. Clos, A. Dadgar, A. Krost, U. Haboeck, and A. Hoffman, *J. Appl. Phys.* **99**, 123518 (2006).
- [19] E. Feltin, B. Beumont, P. Vennéguès, M. Vaille, p. Gibart, T. Riemann, J. Christen, L. Dobos, and B. Pécz, *J. Appl. Phys.* **93**, 182 (2003).
- [20] T. Gehrke, K. J. Linthicum, E. Preble, P. Rajagopal, C. Ronning, C. Zorman, M. Mehregany, and R. F. Davis, *J. Electron. Mater.* **29**, 306 (2002).
- [21] A. Watanable, T. Takeuchi, and K. Hirosawa, *J. Cryst. Growth* **128**, 391 (1993).
- [21] A. Watanable, T. Takeuchi, and K. Hirosawa, *J. Cryst. Growth* **128**, 391 (1993).
- [22] A. Ohtani, K. S. Stevens, and R. Beresford, *Appl. Phys. Lett.* **65**, 61 (1994).
- [23] P. Kung, A. Saxler, X. Zhang, D. Walker, T. C. Wang, I. Ferguson, and M. Razeghi, *Appl. Phys. Lett.* **66**, 2958 (1995).

- [24] M. Godlewski, J. P. Bergmann, B. Monemar, U. Rossner, and A. Barski, *Appl. Phys. Lett.* **69**, 2089 (1996).
- [25] J. M. Redwing, J. S. Flynn, M. A. Tischler, W. Mitzchel, and A. Saxler, *Mater. Res. Soc. Symp. Proc.* **395**, 201 (1996).
- [26] F. Widmann, B. Daudin, G. Feuillet, Y. Samson, M. Arlery, and J. L. Rouviere, *MRS Internet J. Nitride Semicond. Res.* **2**, 20 (1997).
- [27] H. P. D. Schenk, E. Feltin, M. Laugt, O. Tottreau, P. Vennegues, and E. Dogheche, *Appl. Phys. Lett.* **83**, 5139 (2003).
- [28] K. Hirosawa, K. Hiramatsu, N. Sawaki, and I. Akasaki, *Jpn. J. Appl. Phys.* **32**, L1039 (1993).
- [29] T. Soga, S. Hattori, S. Sakai, M. Takeyasu, and M. Umeno, *J. Appl. Phys.* **57**, 4578 (1985).
- [30] A. Georgakilas, and A. Christou, *J. Appl. Phys.* **76**, 7332 (1994).

### **3.Demonstration on GaN-based light emitting diodes grown on 3C-SiC/Si(111)**

#### **3.1 Introduction**

GaN based optoelectronic devices, including light-emitting diodes (LEDs), grown on Silicon (Si) substrates have been attractive since the last century because of several benefits, such as low manufacturing cost, large size, good thermal conductivity, and integration potential. However, there are some issues regarding the quality of GaN epilayers grown on Si. For instance, there is a large mismatch in the lattice constants up to 17% and as much as 116% difference in the thermal expansion coefficients between the GaN epilayer and Si substrate. In the past, many methods have been suggested to improve the crystalline quality and light output power by applying novel growth techniques, such as using low-temperature AlN and  $\text{Si}_x\text{N}_y$  interlayer [1], or growth on patterned Si substrate [2]. Meanwhile, some researchers have focused on enhancing the light extraction efficiency by using distributed Bragg reflector [3], or micro-roughening of p-GaN surface [4]. Recently, Cuong et al. [5] have reported that the fabrication of micro-pit LEDs constructed on wet-etched patterned sapphire substrate (PPS), has simultaneously improved both the epitaxial layer quality and light extraction efficiency. Previously, it was also proved that, using 3C-SiC as an intermediate layer (IL) could improve the quality of the GaN grown on Si [6-8]. Consequently, GaN based high electron mobility transistors [9] and Schottky diodes [10] were realized by using IL of 3C-SiC. However, until now, the demonstration of GaN based LEDs grown on Si using 3C-SiC IL has not been reported.

In this work, the effect of 3C-SiC IL on the structural property and device performance in GaN-based LEDs grown on Si by MOCVD has been reported. The quality of the epitaxial layers was found to be improved by using 3C-SiC IL, which thereby leads to more than two times enhancement in the light output power when comparing to those devices without 3C-SiC IL.

### 3.2 Experiment

Prior to the device growth by MOCVD, the Si substrate was carbonized through annealing in an atmosphere of propane at 1100 °C, which resulted in the formation of a thin (<50 nm) crystalline 3C-SiC that serves as a template for the 3C-SiC growth [11]. Subsequently, a thicker layer of 3C-SiC IL was obtained on the Si (111) substrate using silane ( $\text{SiH}_4$ ) and propane ( $\text{C}_3\text{H}_8$ ) as the precursors at the same temperature in low pressure ( $10^4$  Pa) [12]. The 3C-SiC crystal polarity was Si polarity [13], and the total thickness was approximately 700 nm. Over the template of 3C-SiC/Si(111), InGaN-based multiple-quantum wells (MQWs) LED structure was grown by MOCVD using a Taiyo Nippon Sanso SR2000 system. Trimethylgallium (TMG), trimethylindium (TMIIn) and ammonia ( $\text{NH}_3$ ) were used as sources for gallium, indium and nitrogen, respectively. Monosilane ( $\text{SiH}_4$ ) diluted in hydrogen was used as n-type dopant, and the p-type dopant was bis-cyclopentadienyl magnesium ( $\text{Cp}_2\text{Mg}$ ). Before the growth of LED structure, a buffer layer (BL) consisting of an AlN layer and an n-AlGaN layer was grown at 1000 °C [14]. Then, 20 pair AlN/GaN (5/20 nm) strained-layer superlattice (SLS) layers and a 200 nm thick n-GaN layer were grown at 1080 °C. Finally, an undoped 15 period MQWs consisting of 1.5 nm thick  $\text{In}_{0.16}\text{Ga}_{0.84}\text{N}$  wells and 10 nm thick  $\text{In}_{0.01}\text{Ga}_{0.99}\text{N}$  barriers, a 20 nm thick p-AlGaN layer at 780 °C,

and a 200 nm thick p-GaN cap layer at 1080 °C were grown successively. For comparison, a sample was grown directly on Si substrate without 3C-SiC IL by the identical growth conditions. For the convenience of following discussion, the two samples are denoted as sample A (without 3C-SiC IL) and sample B (with 3C-SiC IL).

The surface morphology was analyzed using atomic force microscopy (AFM). In order to confirm the crystalline quality of epitaxial layers, high-resolution x-ray diffraction (HR-XRD) (Philips X’Pert Epitaxy), and transmission electron microscopy (TEM) (JEM-2010F) measurements were performed. The top-emitting LEDs with a chip size of  $500 \times 500 \mu\text{m}^2$  were fabricated using a standard process. In the fabrication procedure of LEDs, firstly, the Mg acceptors were activated by furnace annealing in nitrogen atmosphere at 800 °C for 25 min. Then, the thin Ni/Au (6/12 nm) transparent metals were formed on p-GaN layer by the electron-beam evaporation and annealed in air ambient at 600 °C for 3 min. Subsequently, the Ni/Au (5/60 nm) p-type contact electrode was deposited and annealed in air ambient at 450 °C for 90 s. Finally, the n-type ohmic contact was made on the backside of Si substrate from the AuSb/Au (20/100 nm) and annealed in nitrogen atmosphere at 320 °C for 30 s. Figure 3. 1 shows the schematic structure of the LEDs used in this study. The LEDs were characterized using an on-wafer configuration. Current-voltage ( $I-V$ ) measurements were carried out using a semiconductor parameter analyzer (Agilent 4155C). Electroluminescence (EL) spectra and light output power-current ( $L-I$ ) were measured at room temperature using an integrated sphere detector (Otsuka Electronics MPCD-7000).

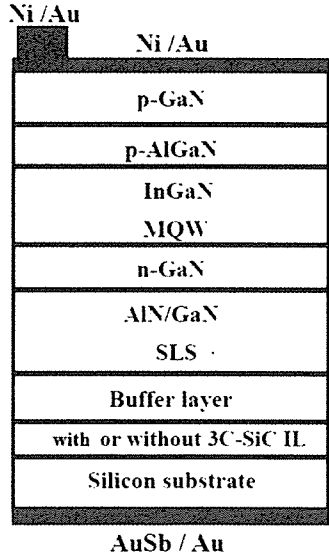


Fig. 3.1. Schematic structure of GaN-based LEDs on Si substrate with or without 3C-SiC IL.

### 3.3 Results and discussion

The two samples in this study are crack-free, with mirror-like surface. AFM images of p-GaN surface for sample A and B are shown in Fig. 3. 2. Some small pits can be observed in both samples. The formation of pit is common in the planar growth of InGaN/GaN MQWs due to the large lattice mismatch [15]. It can be found that the pit density of sample B is lower than that of sample A. In addition, when the scan areas are  $3 \times 3$  and  $1 \times 1 \mu\text{m}^2$ , the root-mean square roughness of sample A are 0.67 and 0.25 nm, and those of sample B are 0.43 and 0.12 nm, respectively.

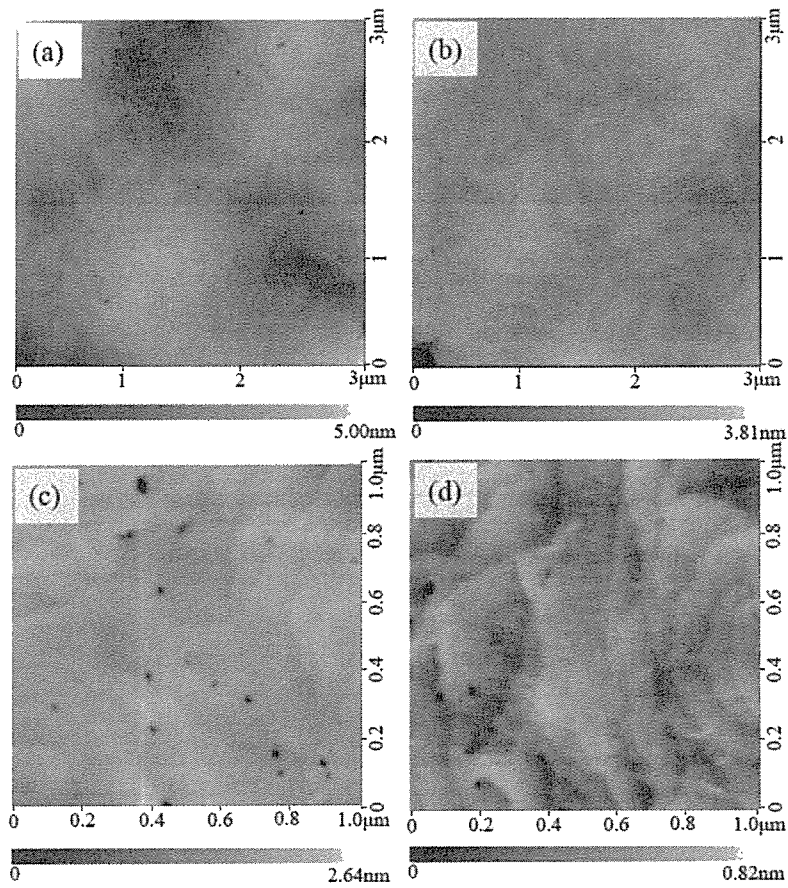


Fig. 3.2. AFM images of p-GaN surface for sample A ( (a) and (c) ) and sample B ( (b) and (d) ). The scan area of (a) and (b) is  $3 \times 3 \mu\text{m}^2$ . For (c) and (d), the scan area is  $1 \times 1 \mu\text{m}^2$ .

Figure 3.3(a) shows GaN (0002)  $\omega$ -2 $\theta$  scans of sample A and B. The strongest peak in each spectrum arises from GaN epitaxial layer. Several distinct satellite peaks from AlN/GaN SLS can be observed on both sides of GaN-peak, and the high-order fringes indicate the superior crystalline quality of SLS structure with sharp interfaces. Based on the positions of fringe peaks, the calculated average thicknesses of SLS period are 23.6 and 25.3 nm for sample A and B, respectively, close to the designed value (25 nm). In addition, it is found that the diffraction peak at  $17.83^\circ$  (0.2579 nm lattice constant) in sample B is stronger than that of sample A. It is believed that this peak

originates from the 3C-SiC (111) IL. The position at  $41.36^\circ$  (0.2181 nm lattice constant) corresponds to the peak of 3C-SiC (002)  $2\theta-\omega$  scan of sample B is also shown in the inset of Fig. 3. 3(a). Figure 3. 3(b) shows GaN (0002) and  $(10\bar{1}2)$  rocking curves of the two samples. The full width at half-maximum of (0002) are 1310 and 991 arcsec, and those of  $(10\bar{1}2)$  are 1836 and 1464 arcsec for sample A and B, respectively.

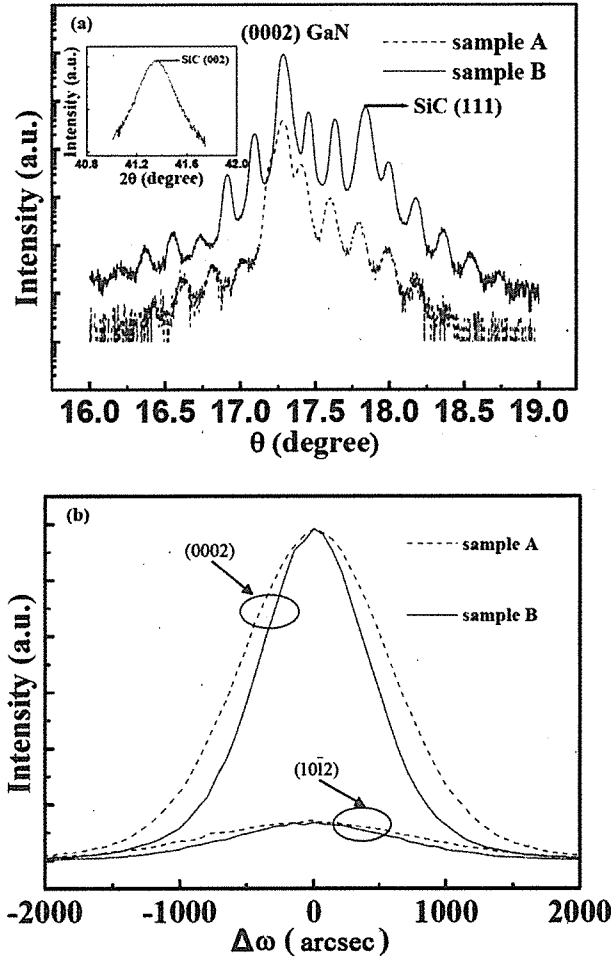


Fig. 3. 3. (a) HR-XRD of  $\omega$ - $2\theta$  scans of GaN (0002) for sample A and B. The inset shows the  $2\theta-\omega$  scan of SiC (002). (b) HR-XRD of  $\omega$ -scans of GaN (0002) and  $(10\bar{1}2)$  for sample A and B.

During the MOCVD growth, strain can be relieved by the 3C-SiC IL because of the less lattice mismatch (3%) between (0001) GaN and (111) 3C-SiC [15]. It is

reasonable that the tensile stress in GaN films with 3C-SiC IL can be reduced to half of that of GaN films without 3C-SiC IL [6,16], resulted from the reduction of thermal expansion coefficient from 116% (between GaN and Si) to 24% (between GaN and 3C-SiC). Consequently, a higher crystalline quality GaN epitaxial layer was realized by utilizing 3C-SiC as IL [6,15]. Figure 3. 4 shows cross-sectional TEM bright-field images of the two samples. Threading dislocations (TDs) in the buffer and the SLS layers of sample A can be observed, while the corresponding TDs in sample B were somewhat suppressed. Moreover, as can be seen in the other layers, including n-GaN, MQWs and p-GaN, the threading dislocation density (TTD) of sample B is lower than that of sample A. In particular, the average TTD in n-GaN of sample A and B are calculated to be approximately  $9.7 \times 10^9$  and  $2.5 \times 10^9 \text{ cm}^{-2}$ , respectively. These results are consistent with aforementioned data of XRD. In addition, as shown in Fig. 3. 5, a number of V-groove defects exist in the region close to the interfaces between the BL and the initial SLS layers in sample A, while the corresponding interfaces are very smooth in sample B. Therefore, it is believed that a significant improvement in the crystalline quality of the epitaxial layers can be realized by using the 3C-SiC IL.

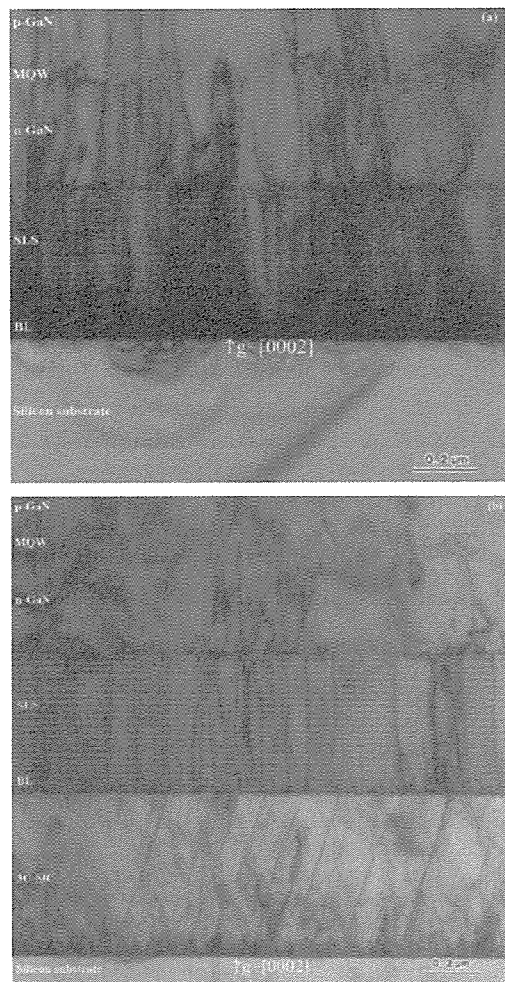


Fig. 3.4. Cross-sectional TEM bright-field images of epitaxial structure for sample A (a) and B (b).

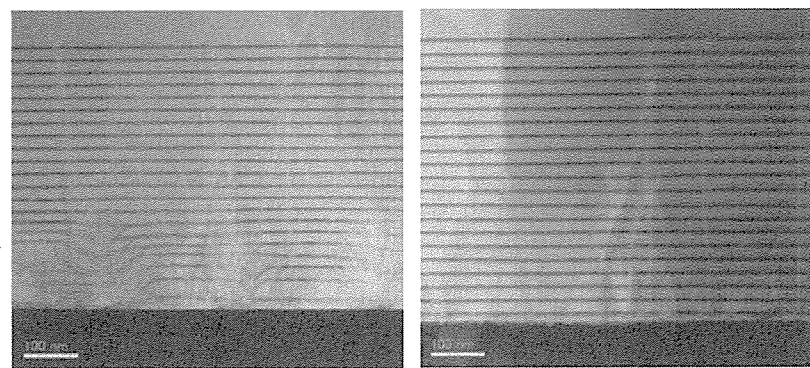


Fig. 3.5. Cross-sectional STEM images of the AlN/GaN SLS layers for sample A (left) and B (right).

The forward  $I$ - $V$  curves of the two samples are shown in Fig. 3. 6. The operating voltage of 3.7 and 3.9 V were obtained at the injection current of 20 mA for sample A and B, respectively. From the  $I$ - $V$  slope, the series resistances of sample A and B are derived to be 34 and 47  $\Omega$ , respectively. It should be noted that using 3C-SiC as IL resulted in a slight higher operation voltage and a higher series resistance due to the 3C-SiC IL. Room temperature EL spectra of the two samples under a drive current of 20 mA are shown in the inset of Fig. 3. 6. The EL peaks are at 480 and 467 nm for sample A and B, respectively.

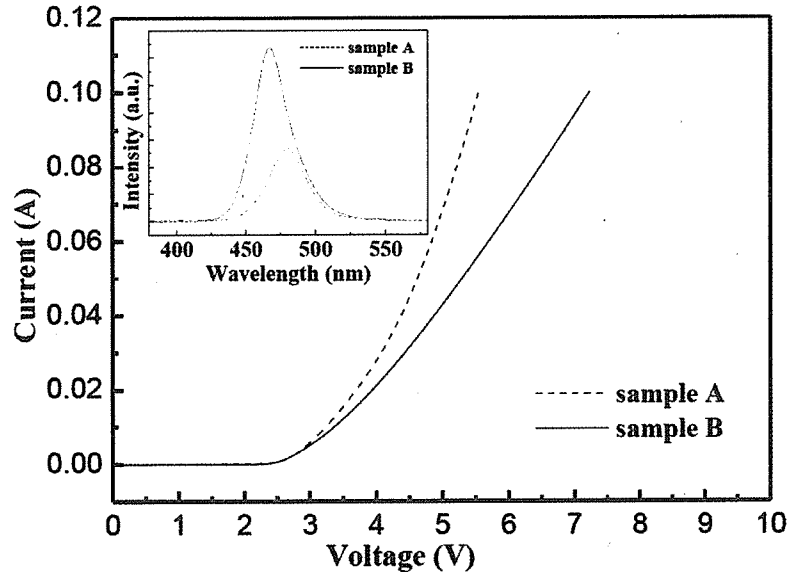


Fig. 3.6. Forward  $I$ - $V$  characteristics of LEDs for sample A and B. The inset shows EL spectra of LEDs at an injection current of 20 mA for sample A and B.

Figure 3. 7 shows the  $L$ - $I$  characteristics of the two samples. At an injunction current of 20 mA, the output power of sample A and B is approximately 50 and 120  $\mu$ W, respectively. The result indicates that more than 200% enhancement in the output power has been achieved by using 3C-SiC as IL. The enhanced light output power is attributed to the lower pit density on the sample surface, the flat interfaces of SLS, and the higher

crystalline quality of GaN epitaxial layers, as mentioned above. It is well known that various compressive strain-relief defects, such as pits, V-groove defects and TDs might be generated during the growth [17]. These defects act as nonradiative recombination centers and/or paths for current leakage, which will deteriorate the device performance [18]. The inset of Fig. 3. 7 is the image of emission from sample B at 5 mA under normal room light condition, which reveals crack-free and uniform emission.

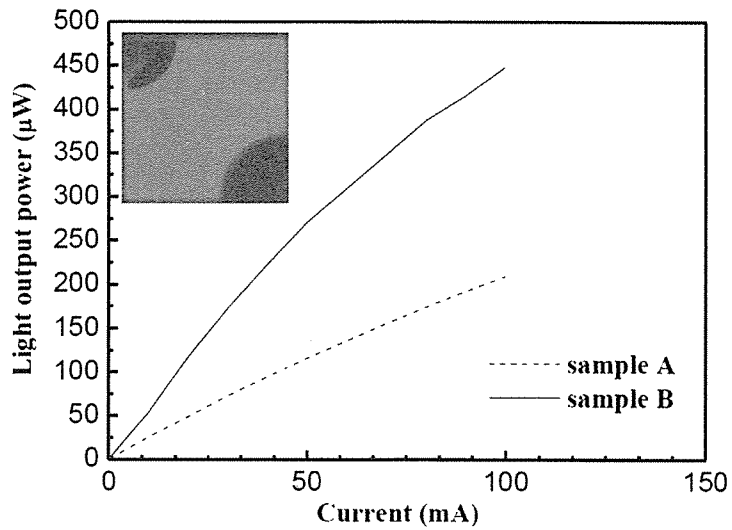


Fig. 3.7.  $L$ - $I$  characteristics of LEDs for sample A and B. The inset shows the image from sample B which was operated at an injection current of 5 mA.

### 3.4 Conclusions

In summary, the GaN-based LEDs on Si substrate by using 3C-SiC as IL has been demonstrated. The effect of 3C-SiC IL on the characteristics of LED has been investigated. The addition of 3C-SiC IL has resulted in the improved GaN crystalline quality, the better interfaces between the buffer and initial SLS layers, and the smoother morphology of the sample surface. As a consequence, the device with 3C- SiC IL showed an enhanced light output power by a factor of 2.4 at a drive current of 20 mA.

The superior device performance was attributed to the improvement in the structural properties, which were clarified by the AFM, XRD, and TEM measurements. This work implies that using 3C-SiC as IL is one of the effective methods for enhancing the light output power of LEDs grown on Si substrate. It will also be of interest for a further study of GaN-based optoelectronic device grown on Si.

## References

- [1] A. Dadgar, M. Poschenrieder, J. Bläsing, O. Contreras, F. Bertram, T. Riemann, A. Reiher, M. Kunze, I. Daumiller, A. Krtschil, A. Diez, A. Kaluza, A. Modlich, M.Kamp, J. Christen, F. A.Ponce, E. Kohn, and A. Krost, *J. Cryst. Growth* **248**, 556 (2003).
- [2] B. S. Zhang, H. Liang, Y. Wang, Z. H. Feng, K. W. Ng, and K. M. Lau, *J. Cryst.Growth* **298**, 725 (2007).
- [3] H. Ishikawa, K. Asano. B. Zhang, T. Egawa, and T. Jimbo, *Phys. stat.sol. (a)* **201**, 2653 (2004).
- [4] C. Huh, K. S. Lee, E. J. Kang, and S. J. Park, *J.Appl. Phys.* **93**, 9383 (2003).
- [5] T. V. Cuong, H. S. Cheong, H. G. Kim, H. Y. Kim, C. H. Hong, E. K. Suh, H. K. Cho, and B. H. Kong, *Appl. Phys. Lett.* **90**, 131107 (2007).
- [6] J. Komiyama, Y. Abe, S. Suzuki, and H. Nakanishi, *J.Appl. Phys.* **100**, 033519 (2006).
- [7] A. Yamamoto, T. Yamauchi, T. Tanikawa, M. Sasase, B. K. Ghosh, A. Hashimoto,

and Y. Ito. *J. Cryst. Growth* **261**, 266 (2004).

[8] H. M. Liaw, R. Venugopal, J. Wan, and M. R. Melloch, *Solid-State Electron.* **45**, 1173 (2001).

[9] Y. Cordier, M. Portail, S. Chenot, O. Tottreau, M. Zielinski, and T. Chassagne, *J. Cryst. Growth* **310**, 4417 (2008).

[10] J. Komiyama, Y. Abe, S. Suzuki, T. Kita, and H. Nakanishi, *J. Cryst. Growth* **275**, e1001 (2005).

[11] S. Nishino, J. A. Powell, and H. A. Will, *Appl. Phys. Lett.* **42**, 460 (1983).

[12] J. Komiyama, Y. Abe, S. Suzuki, and H. Nakanishi, *J. Appl. Phys.* **100**, 033519 (2006).

[13] T. Egawa, B. Zhang, and H. Ishikawa, *IEEE Electron Device Lett.* **26**, 169 (2005).

[14] F. Lin, N. Xiang, P. Chen, S. Y. Chow, and S. J. Chua, *J. Appl. Phys.* **103**, 043508 (2008).

[15] J. Komiyama, Y. Abe, S. Suzuli, and H. Nakanishi, *Appl. Phys. Lett.* **88**, 091901 (2006).

[16] T. Kozawa, T. Kachi, H. Kano, H. Nagase, N. Koide, and k. Manabe, *J. Appl. Phys.* **77**, 4389 (1995).

[17] H. K. Cho, J. Y. Lee, G. M. Wang, and C. S. Kim, *Appl. Phys. Lett.* **79**, 215(2001).

[18] C. Netzel, H. Bremers, L. Hoffmann, D. Fuhrmann. U. Rossow, and A. Hangleiter, *Phys. Rev.B* **76**, 155322 (2007).

## **4. Improvement of GaN-based light emitting diodes by altering n-GaN thickness**

### **4.1 Characterization of GaN-based light emitting diodes grown on 4-in. Si(111) substrate**

#### **4.1.1 Introduction**

GaN and its related alloys have been investigated extensively in optoelectronic and microelectronic devices since the last century [1-2]. Nowadays GaN-based in the range of ultraviolet to visible light emitting diodes (LEDs) are commercially available. Those device structures almost have been grown on sapphire or SiC substrates. However, in the case of a larger scale fabrication, employing those substrates will be hindered because of their size and high costs. For solving this issue, as one of the effective methods, the growth of LEDs on highly conducting 4- to 12-in. silicon (Si) substrates has been proposed. Moreover, choosing Si as substrate can offer lots of advantages, such as good thermal conductivity, the simplicity of process, and the possibility of integration of Si electronics on the same chip [3]. On the other hand, regarding the GaN epitaxial growth on Si, it is still a challenging issue to modulate tensile stress, resulting from the large mismatches in the lattice constants and thermal expansion coefficients between the GaN layer and Si substrate. Therefore, it always results in the occurrence of cracks and high density threading dislocations [4]. Nevertheless, including our group, many demonstrations of LEDs grown on Si have been reported [2,5-9]. At the same time, it can be found that, with respect to the structure characterization, such as cross-section scanning electron microscopy (SEM)

and transmission electron microscopy (TEM), only some few related results have been presented in those reports until now. Actually, in order to improve the device performance, it is significantly necessary to get some important information through some corresponding accurate measurements.

In this study, the GaN-based LEDs grown on 4-in. Si(111) substrate by MOCVD have been successfully fabricated. The structural property of the sample has been investigated by high-resolution X-ray diffraction (HR-XRD), SEM, and TEM measurements. Based on these results, some consistent correlations have been discussed. In addition, the device performance in the light output power has been characterized. The maximum output power of 3.3 mW and a saturation operating current of 400 mA imply the good performance of LED grown on 4-in. Si(111) substrate.

#### 4.1.2 Experiment

A commercial MOCVD reactor system (Nippon Sanso SR-4000) was used for the epitaxial growth of InGaN-based multiple-quantum wells (MQWs) LEDs structure. Prior to the growth of LEDs structure, a buffer layer consisting of a 5 nm n-AlN layer and a 20 nm n-AlGaN layer was grown. Then, 100 pair n-AlN/GaN (5/20 nm) strained-layer superlattice (SLs) layers and n-GaN layer were grown. Finally, an undoped 10 period MQWs consisting of 4 nm  $\text{In}_x\text{Ga}_{1-x}\text{N}$  wells and 8 nm  $\text{In}_y\text{Ga}_{1-y}\text{N}$  barriers, a 20 nm p-AlGaN layer and a 100 nm p<sup>+</sup>-GaN cap layer were grown successively. The detailed growth conditions can be also found in our previous report [10]. Here, it should be noted that, in this sample during the epitaxial growth of 2  $\mu\text{m}$  n-GaN, there are no any interruption layers, such as AlN or SiN layer. In order to confirm the crystalline quality

of epitaxial layers, the measurements of HR-XRD (Philips X’Pert Epitaxy), cross-section SEM (Hitachi SU-70), and TEM (JEM-2010F, 200 kV) were performed.

The top-emitting LEDs with a chip size of  $500 \times 500 \mu\text{m}^2$  were fabricated using a standard process. In the main LEDs processing, there are multiple-mask photo-lithography, reactive ion etching, metal evaporation and annealing. The details and the schematic structure of the LEDs can be referred to our previous report [11]. No roughening or LED die shaping was used in this study to enhance the extraction efficiency. The LEDs were characterized using an on-wafer configuration. Light output power was measured under the conditions of room temperature and various direct current (DC) using an integrated sphere detector (Otsuka Electronics MPCD-7000).

#### 4.1.3 Results and discussion

The sample in this study is crack-free, and shows mirror-like surface for the whole wafer. Figure 4. 1 shows GaN(0002) XRD  $2\theta-\omega$  scan of the sample. The strongest peak arises from the GaN layer. Also, it is interesting that two kinds of fringe peaks simultaneously appear on the both sides of the major GaN peak, which indicates the good interface and layer periodicity. It should be noted that a position of an average Indium composition of the InGaN layers in the MQWs is indicated by the 0th peak of MQWs. Using the equation  $D = n\lambda/2(\sin_{n\text{th}} - \sin_{0\text{th}})$  [12], the period thickness can be determined. For example, the average period thickness of MQWs can be calculated to be 13.5 nm, and which is close to the designed value (12 nm). At the same time, the thickness of one period SLs has been calculated to be 19.5 nm. Therefore, it can be concluded that one kind of well-defined satellite diffraction peaks to high orders (until  $\pm 6$ ) originate from the SLs, and another one as marked by arrow, which arise from

MQWs. Zhang et al. have reported the similar results [13]. Comparing with those date, however, the SLs and MQWs relative intensity of our sample have become much stronger, which are mainly attributed to the more SLs pairs and higher crystalline quality of MQWs.

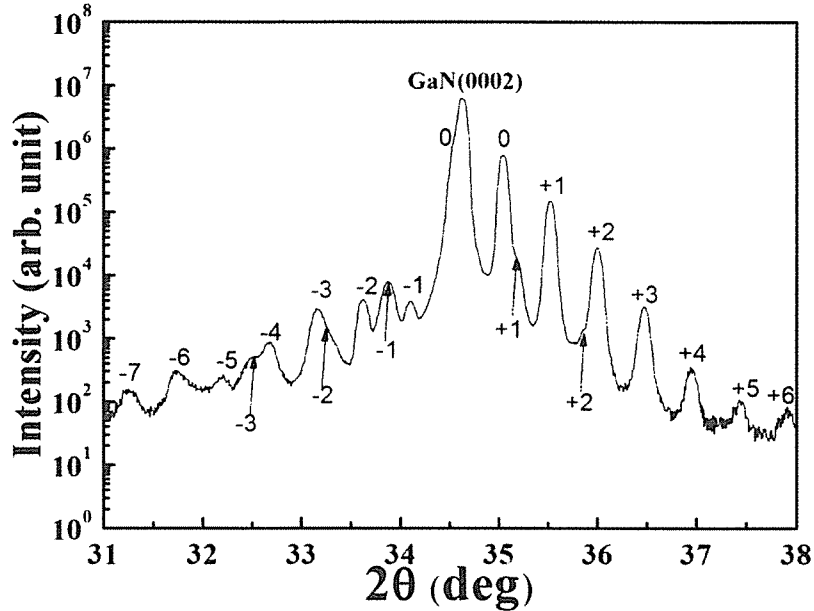


Fig. 4. 1. HR-XRD in GaN(0002)  $\omega$ - $2\theta$  scan of sample. In this figure, the fringe peaks indicated by the number from -7 to +6 originate from the SLs layers. And the fringe peaks indicated by the arrow with the number from -3 to +2 arise from the MQWs layers. The 0th peak (left side to the GaN peak) of MQWs typically indicates a position of an average In composition in the MQWs. And, the 0th peak (right side to the GaN peak) of SLs typically indicates a position of an average Al composition in the SLs.

Figure 4. 2 shows the cross-section images for the SLs layers of the sample under the magnifications of 35 and 100 K. The considerably smooth interfaces can be clearly observed in the area of SLs. This result is consistent with the aforementioned date of HR-XRD. Also, the pairs have been confirmed to be 100, it is in good agreement with the designed value. Moreover, the thickness of one period SLs from SEM images

is 22.2 nm. However, the discrepancy seems a little large when comparing with the corresponding value (19.5 nm) of XRD, and we suppose that it might result from in-plane distribution of the growth rate, especially for using the larger 4-inch substrate. On the other hand, the cross-section TEM images for the MQWs layers of the sample are shown in Fig. 4. 3. It can be confirmed that 10 period MQWs with one period thickness of 14 nm, the significantly good interfaces as well have been grown. It also coincides with the above result of HR-XRD. Based on these structure characterizations, it can be concluded that, the epitaxial layers of both the SLs and MQWs with the high crystalline quality in this sample have been successfully grown. Therefore, its aforementioned characterizations suggest that the growth of GaN-based LEDs grown on Si should lead to good performance device.

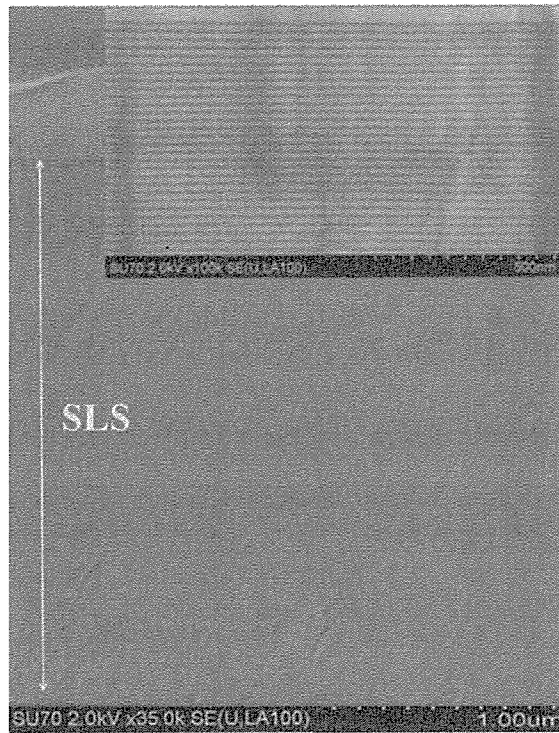


Fig. 4. 2. Cross-section SEM images for the SLs layers of sample under the two magnifications of 35 and 100 K.

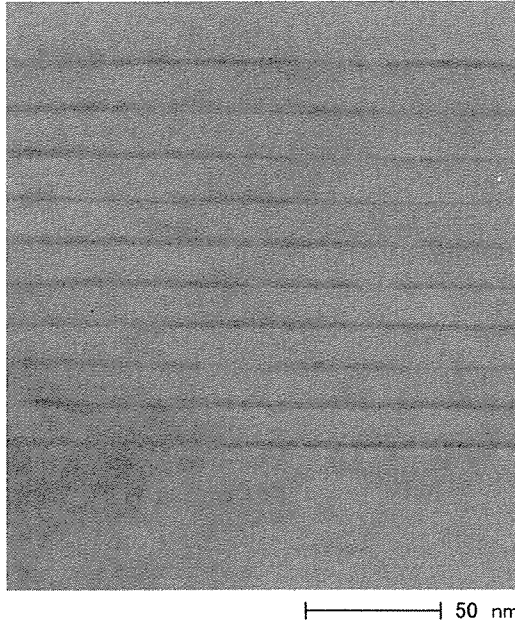


Fig. 4. 3. Cross-section TEM image for the MQWs layers of sample.

The light output power versus various injection current ( $L-I$ ) characteristics of the sample are shown in Fig. 4. 4. It can be clearly seen that the output power of LED increases linearly with the injection current up to 100 mA. And, it still continues to increase steadily. However, the output power starts to saturate and finally reaches at a maximum value of 3.3 mW. Then, it decreases slightly as the injection current is further increased, which is attributed to the thermal dissipation at high injection currents [14]. While the saturation operating current of the sample is 400 mA. In the LEDs structure of this study, the total thickness beneath MQWs is 4.5  $\mu\text{m}$ . It should be noted that only in the SLs layers, the total thickness of the AlN layers reaches to 0.5  $\mu\text{m}$ , these factors including Si substrate have been contributed to the good thermal dissipation. It will further influent on the saturation operating current. Actually, the LED performance in this study is close enough to those in other group (6.3 mW at the saturation current of 500 mA) [15], which has been reported to be also comparable to those in the sapphire substrate case. It is worth noting that, some thermal dissipation technologies, such as bonding on a metal head (as shown in ref. 15), have not been employed in our device.

Therefore, it can be supposed that this device with good performance is mainly attributed to the high quality of epitaxial layer and good thermal conductivity of Si substrate. The inset of Fig. 4. 4 indicates the emission image of the sample under an injection current of 20 mA. It implies bright and uniform light, resulting from active layers of InGaN-based MQWs. From these results, it can be concluded that the LED in this study has exhibited the good optical characteristics. The other device properties, including current-voltage and electroluminescence, can be found in our previous report [10].

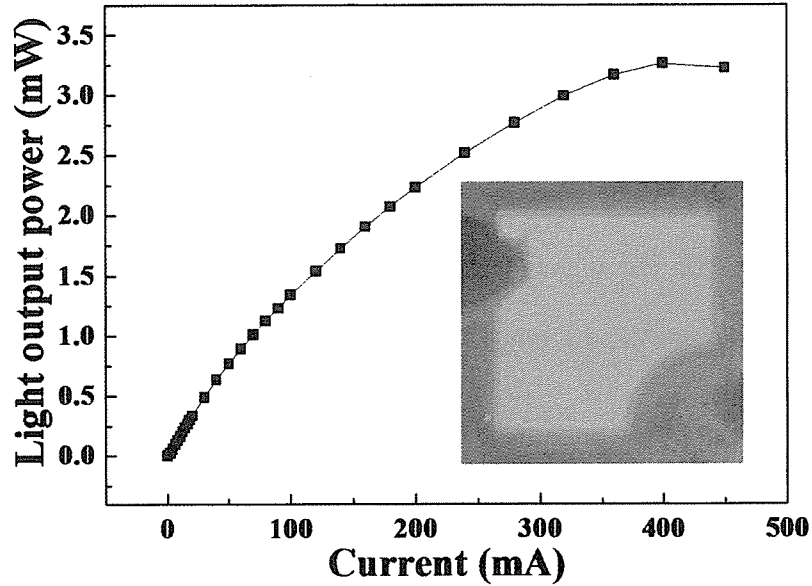


Fig. 4. 4. Light output power of sample as a function of injection DC current. The inset shows the emission image (@ 20 mA).

As well known, comparing to the LEDs grown on sapphire, the LEDs on Si show the relative lower light output power. It often results from several typical factors, such as, the light absorption of Si substrate, the crystalline quality of epitaxial layers, and the device structure. In particular, due to absorption in the Si substrate, the light extraction efficiency for device on Si (3.74%) is even lower than on sapphire (5.4%)

[15]. This indicates the need for substrate removal methods should be implemented in device processing. Zhang et al. have used wafer bonding and selective lift-off technique to eliminate not only substrate absorption but also the large band offset between the AlN buffer layer and the Si substrate [16]. In that report, the optical power has been revealed an enhancement of 47% compared to the LED before substrate removal. Although those influence issues exist, it can be also expected that the performance of LEDs grown on Si will be further improved by means of some new effective approaches in the future.

## **4.2 High performance of GaN-based light emitting diodes grown on 4-in. Si(111) substrate**

### **4.2.1 Introduction**

GaN and related alloys are one of the promising materials for applications in optoelectronic and microelectronic devices [1-2]. Nowadays GaN-based blue-green and white light emitting diodes (LEDs) are commercially available almost on sapphire and SiC substrates. For a larger scale fabrication, however, those substrates are limited because of their size and higher costs. In order to solve this issue, one of the effective approaches is to grow LEDs on highly conducting 4- to 12-in. silicon (Si) substrates. Moreover, choosing Si as substrate can offer a great deal of advantages, such as the good thermal conductivity, the simplicity of process, and the possibility of integration of Si electronics on the same chip [3]. On the other hand, in terms of the GaN epitaxial growth on Si, it is well known that the most challenging issues are to relieve tensile stress due to the large thermal expansion coefficient and lattice constant mismatches between GaN layer and Si substrate, which always result in the occurrence of cracks

and high density threading dislocations [4]. Nevertheless, the demonstrations of LEDs grown on Si have been reported by some groups [2,5-9]. Several approaches have been previously attempted to control the strain and minimize the cracks, such as using AlN/GaN multilayers with a thin AlN/AlGaN buffer layer [2-3], the insertion of AlGaN/GaN superlattice structure [17], employing low-temperature AlN and  $\text{Si}_x\text{N}_y$  interlayer[5,18] , and so on [7-8,11]. In those previous demonstrations, LEDs structures have been grown almost on 2-in. Si substrates until now [2,5,8,17], except some few groups have used 6-in. Si substrates [6]. Because the growth of thick GaN will be more difficulty with increasing the size of Si substrate due to the larger strain, which further leads to a bigger value of curvature and induces some cracks. In addition, with respect to the external quantum efficiency (EQE), some few data have been reported. Fenwick et al. have presented it with a low value of 0.1% [19]. So far of our knowledge, although the GaN-based hetero-junction field effect transistors and high electron mobility transistors have been demonstrated on 4-in. Si substrate [20-21] , there have been no previous demonstrations of the LEDs grown on the same diameter Si substrate.

In this work, we have successfully fabricated the GaN-based LEDs grown on 4-in. Si(111) substrate by metal-organic chemical vapor deposition (MOCVD) for the first time. The properties of samples have been investigated in detail by high-resolution X-ray diffraction (HR-XRD), current-voltage ( $I-V$ ), electroluminescence (EL), and light output power-current ( $L-I$ ) measurements. It is found that the light output power of the LEDs has been enhanced by two times with increasing n-GaN layer thickness. Regarding the enhancement of the optical power, some mechanisms have also been discussed between the structural and device property.

#### 4.2.2 Experiment

A commercial MOCVD reactor system (Nippon Sanso SR-4000) was used for the epitaxial growth of InGaN-based multiple-quantum wells (MQWs) LEDs structure. Trimethylgallium (TMG), trimethylindium (TMIIn), and ammonia ( $\text{NH}_3$ ) were used as sources for gallium, indium and nitrogen, respectively. Monosilane ( $\text{SiH}_4$ ) diluted in hydrogen was used as n-type dopant, and the p-type dopant was biscyclopentadienyl magnesium ( $\text{Cp}_2\text{Mg}$ ). Prior to the growth of LEDs structure, a buffer layer (BL) consisting of a 5 nm n-AlN layer and a 20 nm n-AlGaN layer was grown at 1030 °C. Then, 100 pair n-AlN/GaN (5/20 nm) strained-layer superlattice (SLS) layers and n-GaN layer were grown at 1130 °C. Finally, an undoped 10 period MQWs consisting of 4 nm  $\text{In}_x\text{Ga}_{1-x}\text{N}$  wells and 8 nm  $\text{In}_y\text{Ga}_{1-y}\text{N}$  barriers at 800 °C, a 20 nm p-AlGaN layer and a 100 nm p<sup>+</sup>-GaN cap layer at 1030 °C were grown successively. For comparison, two samples were prepared, in which only n-GaN thicknesses were different. The thicknesses of n-GaN were 2 and 1 μm in sample A and B, respectively. In order to confirm the crystalline quality of epitaxial layers, HR-XRD (Philips X’Pert Epitaxy) measurement was performed.

The top-emitting LEDs with a chip size of  $500 \times 500 \mu\text{m}^2$  were fabricated using a standard process. Main fabrication procedure of the LEDs included multiple-mask photo-lithography, reactive ion etching, metal evaporation and annealing. The details can be referred to our previous report [11]. Figure 4. 5 shows the schematic structure of the LEDs used in this study. The LEDs were characterized using an on-wafer configuration. *I-V* measurement was carried out using a semiconductor parameter analyzer (Agilent 4155C). EL spectra and light output power were measured under the

conditions of room temperature and various direct current using an integrated sphere detector (Otsuka Electronics MPCD-7000).

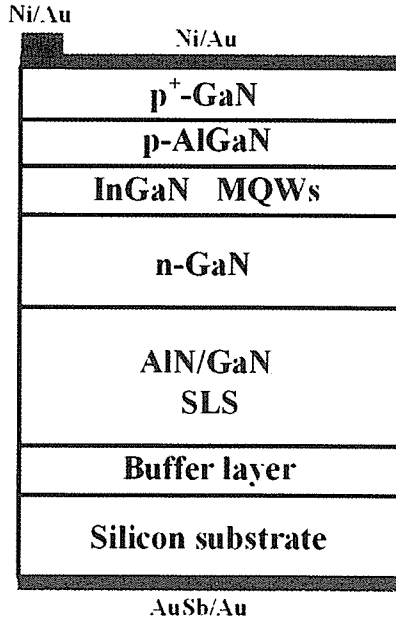


Fig. 4. 5. Schematic structure of GaN-based LEDs.

#### 4.2.3 Results and discussion

Two samples in this study are crack-free, and show mirror-like surface for the whole wafer. Figure 4. 6 shows GaN(0002) and (10-12) XRD  $\omega$ -scans rocking curves of samples A and B. The full width at half maximum (FWHM) of (0002) are 626 and 916 arcsec, and those of (10-12) are 1464 and 1604 arcsec for samples A and B, respectively. This indicates that there is a significant improvement of GaN epitaxial quality when increasing the thickness of n-GaN. For sample A, the density of screw component threading dislocation (TDs) is calculated to be  $7.9 \times 10^8 / \text{cm}^2$  from the extracted tilt value [22], which is lower by one order of magnitude comparing with our previous results [11]. Therefore, it can be expected that the LEDs with high performance grown on Si will be realized

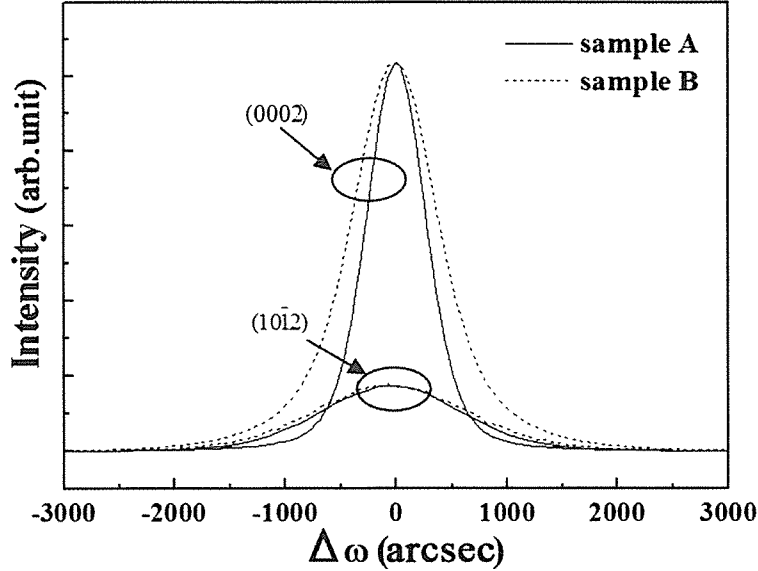


Fig. 4. 6. XRD rocking curves in GaN (0002) and (10-12)  $\omega$ -scans of sample A and B.

The typical  $I$ - $V$  characteristics of the two samples are shown in Fig. 4. 7. At an injection current of 20 mA, the operating voltage of sample A and B is 6.1 and 8.0 V, respectively. For the study of vertical-LED on Si, the electrons injection is carried out from Si substrate into the active layer through the BL and SLS layers. Consequently, the electrons will encounter some large barriers during the injection. And it will also lead to the high turn-on and operating voltages [23]. In addition, the epitaxial quality also influences the electrical property, that is, some TDs are related with the voltage. It should be noted that the results of  $I$ - $V$  are in good agreement with the results of XRD. On the other hand, room temperature EL spectra of sample A under various currents are shown in Fig. 4. 8. The EL peak is centered at 487 nm at the injection current of 20 mA, which corresponds to near band edge luminescence from the optically active region. In addition, it is interesting to note that a few blue-shifts have occurred with increasing the current. This is attributed to the free-carrier-screening and band-filling effects[24].

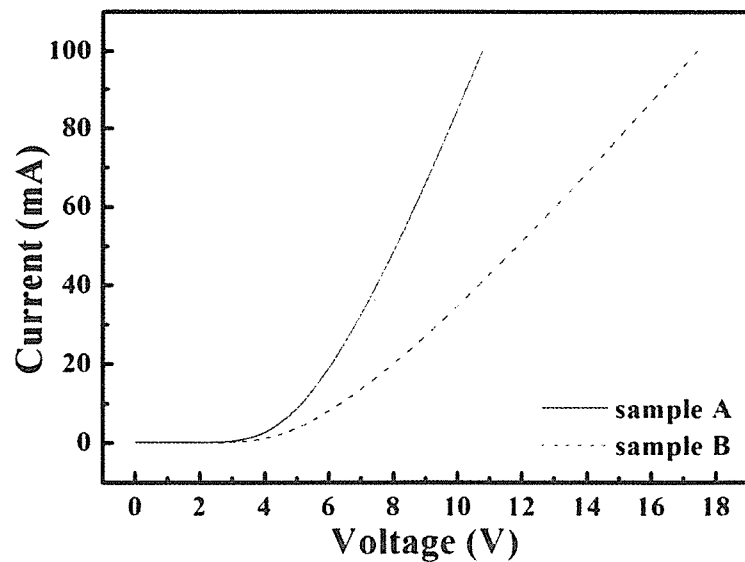


Fig. 4. 7.  $I$ - $V$  characteristics of sample A and B.

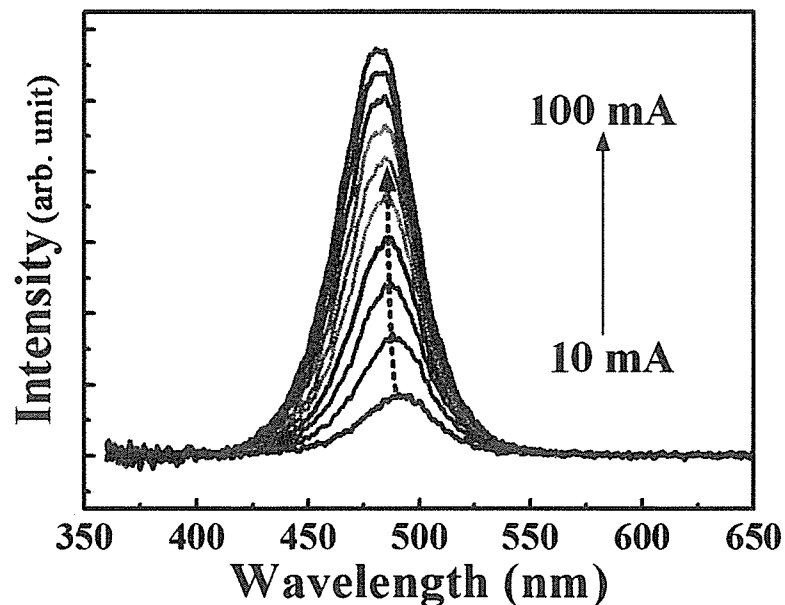


Fig. 4. 8. EL spectra of sample A as a function of injection current, and the blue-shifts of emission peak are indicated by dot line arrow.

Figure 4. 9. shows the typical light output power and EQE versus injection current ( $L$ -EQE- $I$ ) characteristics of samples A and B. It can be seen clearly that the output power of LEDs increases linearly with injection current initially. At the injection current of 20 mA, the output power of sample A and B is 298.3 and 152.4  $\mu$ W,

respectively. This indicates that the increment of sample A has reached near to 200% with comparing to sample B. However, the output power starts to saturate and finally reaches at maximum value, then decreases slightly as the injection current is further increased. It can be observed that the maximum output power of sample A and B is 1.71 and 0.68 mW, respectively. While the saturation operating current of sample A and B is 280 and 170 mA, respectively. From those results, it can be confirmed that the optical power of sample A has been improved by increasing the thickness of n-GaN. The aforementioned data are consistent with the results of XRD and *I-V*.

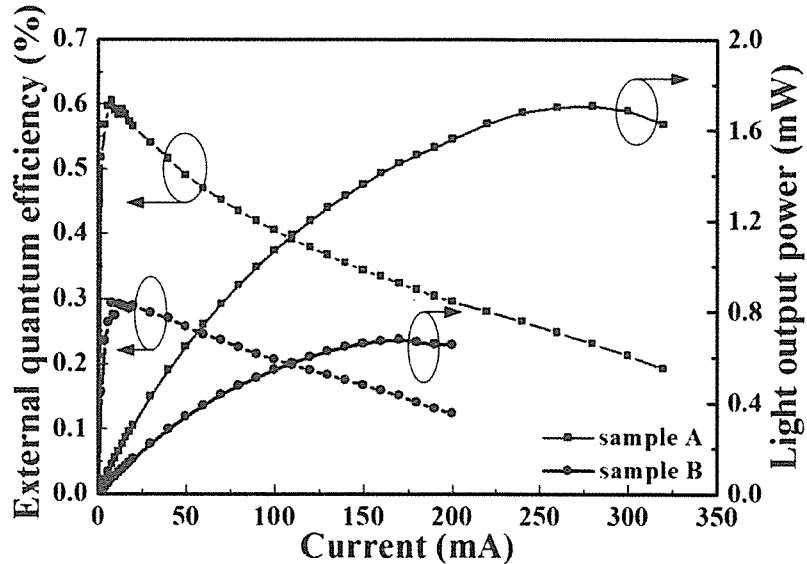


Fig. 4. 9. *L-EQE-I* characteristics of sample A and B as a function of injection current.

Recently, Li et al. have reported that the saturation current of GaN-based LEDs grown on Si was about 170 mA [6]. Comparing with this result, it is worth noting that the corresponding date of sample A is higher by a factor of 1.75. Therefore, it can be speculated that the device with high performance are mainly attributed to the high quality of epitaxial layer and good thermal conductivity of Si substrate. In addition, as shown in Fig. 4. 9, we can find that the maximum EQE of sample A and B is about 0.6 and 0.3%, respectively. These results are well consistent with aforementioned ones. On

the other hand, it can be also found that the efficiency droop is remarkable, resulting from several factors, such as carrier leakage from the active region, Joule heating from the series and parasitic resistances, high polarization and so on [25].

As well known, concerning the LEDs grown on Si, lower light output power comparing to that on sapphire results from several factors, such as, the light absorption by the Si substrate, the quality of GaN, the structural design and growth parameters [8]. Actually, in our study, if the n-GaN thickness is over 2  $\mu\text{m}$ , some cracks will emerge on the device surface. It can be expected to be solved by strain modulation of the optimized SLS. In addition, one of hard issues is distribution controlling in the whole wafer, in particular, for the big size of 4- to 12- in. Si substrate. In this demonstration, the standard deviation of peak position is approximately 12% for the two samples. It can be contributed to the indium fluctuation in the MQWs, which might due to different InGaN-phase segregation. It is well known that bowing values will be larger with increasing the size of Si substrate, and it results from the variation of strain. Moreover, it will result in the distribution of growth temperature of epitaxial layers. Consequently, the indium corporations will not be same in the whole wafer. Despite those above influence issues, it can be believed that the performance of LEDs grown on Si will be improved further by means of some new effective approaches in the near future.

### 4.3 Conclusions

In conclusion, in the section 4.1, the high quality GaN-based LEDs with a 2  $\mu\text{m}$  n-GaN grown on 4-in. Si(111) substrate by MOCVD have been characterized. The sample structural property with the smooth interfaces has been confirmed by XRD, SEM, and TEM measurements. Moreover, the LED with a maximum light output power

of 3.3 mW and a high saturation operating current of 400 mA has been realized. Nevertheless, the characterizations have revealed some important results, which would boost the researchers to further improve the performance of LEDs grown on Si substrate.

On the other hand, in the section 4.2, the feasibility for growing high quality GaN-based LEDs by MOCVD on 4-in. Si(111) substrate have been demonstrated. The structural, electrical, and optical properties of the samples have been systematically clarified. It is demonstrated that the performance of GaN-based LEDs can be improved by increasing the thickness of n-GaN. As a consequent, 1.7 mW output power of LEDs with a high saturation operating current of 280 mA have been fabricated. Therefore, the demonstration revealed some important results, which would promote the device researchers to further improve the performance of LEDs grown on Si substrate.

## References

- [1] S. Nakamura, G. Fasol, and S.J. Pearton: *The Blue Laser Diode: The Complete Story* (Springer, New York, 2000), 2nd ed., and references therein.
- [2] T. Egawa, B. Zhang, and H. Ishikawa: IEEE Electron Device Lett. **26**, 169 (2005).
- [3] T. Egawa, T. Moku, H. Ishikawa, K. Ohtsuka, and T. Jimbo: Jpn. J. Appl. Phys. **41**, L663 (2002).
- [4] H. Ishikawa, G. Y. Zhao, N. Nakada, T. Egawa, T. Jimbo, and M. Umeno: Jpn. J. Appl. Phys. **38**, L492 (1999).
- [5] A. Dadgar, M. Poschenrieder, J. Bläsing, K. Fehse, A. Diez, and A. Krost: Appl. Phys. Lett. **80**, 3670 (2002).
- [6] J. Li, J. Y. Lin, and H. X. Jiang: Appl. Phys. Lett. **88**, 171909 (2006).

- [7] S. Tripathy, V. K. X. Lin, S. L. Teo, A. Dadgar, A. Diez, J. Bläsing, and A. Krost: *Appl. Phys. Lett.* **91**, 231109 (2007).
- [8] B. Zhang, H. Liang, Y. Wang, Z. Feng, K. W. Ng, and K. M. Lau: *J. Cryst. Growth* **298**, 725 (2007).
- [9] C. Mo, W. Fang, Y. Pu, H. Liu, and F. Jiang: *J. Cryst. Growth* **285**, 312 (2005).
- [10] Y. Zhu, A. Watanabe, L. Lu, Z. Chen and T. Egawa: *Jpn. J. Appl. Phys.* **50**, 04DG08 (2011).
- [11] Y. H. Zhu, J. C. Zhang, Z. T. Chen and T. Egawa: *J. Appl. Phys.* **106**, 124506 (2009).
- [12] I. H. Kim, H. S. Park, Y. I. Park, and T. Kim: *Appl. Phys. Lett.* **73**, 1634 (1998).
- [13] B. Zhang, T. Egawa, H. Ishkawa, Y. Liu, and T. Jimbo: *Jpn. J. Appl. Phys.* **42**, L226 (2003).
- [14] D. S. Wuu, W. K. Wang, K. S. Wen, S. C. Huang, S. H. Lin, S. Y. Huang, C. F. Lin, and R. H. Horng: *Appl. Phys. Lett.* **89**, 161105 (2006).
- [15] D. Zhu, C. McAleese, M. Häberlen, C. Salcianu, T. Thrush, M. Kappers, A. Phillips, P. Lane, M. Kane, D. Wallis, T. Martin, M. Astles, N. Hylton, P. Dawson, and C. Humphreys: *J. Appl. Phys.* **109**, 014502 (2011).
- [16] B. J. Zhang, T. Egawa, H. Ishkawa, Y. Liu, and T. Jimbo: *Appl. Phys. Lett.* **86**, 071113 (2005).
- [17] S. Raghvan and J. M. Redwing: *J. Appl. Phys.* **98**, 023514 (2005).
- [18] A. Dadgar, M. poschenrieder, O. Contreras, J. Christen, K. Fehse, J. Bläsing, A. Diez, F. Schlze, T. Riemann, F. A. Ponce, and A. Krost: *Phys. Status Solidi (A)* **192**, 308 (2002).
- [19] W. E. Fenwick, A. Melton, T. Xu, N. Li, C. Summers, M. Jamil, and L. T.

- Ferguson: Appl. Phys. Lett. **94**, 222105 (2009).
- [20] J. D. Brown, R. Borges, E. Piner, A. Vescan, S. Singhal, and R. Therrien: Solid-State Electron. **46**, 1535 (2002).
- [21] J. Selvaraj, S. L. Selvaraj, and T. Egawa: Jpn. J. Appl. Phys. **48**, 121002 (2009).
- [22] Z. T. Chen, K. Xu, L. P. Guo, H. Zhang, and G. Y. Zhang: J. Cryst. Growth **294**, 156 (2006).
- [23] T. Egawa, B. Zhang, N. Nishikawa, H. Ishikawa, and M. Umeno: J. Appl. Phys. **91**, 528 (2002).
- [24] T. Kuroda and A. Tackeuchi: J. Appl. Phys. **92**, 3071 (2002).
- [25] M. H. Kim, M. F. Schubert, Q. Dai, J. K. Kim, E. F. Schubert, J. Piprek, and Y. Park: Appl. Phys. Lett. **95**, 241109 (2009).

## 5. Summary and future work

This report describes the study on the material characterization, fabrication, and evaluation for GaN-based light emitting diodes (LEDs) grown on silicon (111) substrate. In the section 1 to 2, the research background and epitaxial growth of MOCVD have been presented. It is known that the high quality GaN grown on Si is difficult to be achieved, which can be contributed to the large tensile stress induced by the lattice mismatch of 17% different thermal expansion coefficients of 116% and between GaN and Si substrate. In particular, during the cooling to room temperature, it often results in the cracks on the surface and the high threading dislocation density (TDD) in the layers, these are useless for device applications. Especially, these problems are the major obstacle to realize high performance GaN-based LEDs grown on Si(111) substrate. For example, the high TDD quickly degrades the LEDs lifetime, which is critical for application in commercial products. On the other hand, large substrate bowing is also the origin of cracks in the epitaxial layer. In order to obtain crack free layer, which has limited the n-GaN layer thickness with the maximum value of 2  $\mu\text{m}$  in the LEDs structure of this study.

Prior to the growth of layers for GaN-based LEDs, a thin n-AlN nucleation layer and n-AlN/GaN strained-layer superlattice (SLS) has been utilized. In normal growth design of LED, n-type GaN layer, multiple quantum wells (MQWs), and p-type GaN are followed after the aforementioned SLS layers. However, in this conventional design, a part of light emitted from MQWs in the active layer is absorbed by the underlying Si(111) substrate. In these approaches of improving the material, electrical, and optical characteristics of GaN-based LEDs grown on Si(111) substrate,

the templet of 3C-SiC/Si(111) has been employed. In addition, based on increasing the pair of SLS to 100, the n-GaN thickness has been varied. Herein, it should be noted that the size of Si substrate in the latter one is 4-inch.

In the section 3, the GaN-based LEDs on Si substrate by using 3C-SiC as an intermediate layer (IL) have been demonstrated. The effect of 3C-SiC IL on the characteristics of LED has been investigated. The addition of 3C-SiC IL has resulted in the improved GaN crystalline quality, the better interfaces between the buffer and the initial SLS layers, and the smoother morphology of sample surface. As a consequence, the device with 3C-SiC IL showed an enhanced light output power by a factor of 2.4 at a drive current of 20 mA. The superior device performance was attributed to the improvement in the structural properties, which were clarified by AFM, XRD, and TEM measurements. This study implies that using 3C-SiC as IL is one of the effective approaches for enhancing the light output power of LEDs grown on Si substrate. It will also be of interest for a further study of GaN-based optoelectronic device grown on Si.

While, there are two sections in the section 4. In the section 4.1, GaN-based LEDs with a total thickness of 4.8  $\mu\text{m}$  have been grown by metal-organic chemical vapor deposition on 4-in. Si(111) substrate. The structural property has been revealed by the measurements of high-resolution X-ray diffraction, scanning electron microscopy and transmission electron microscopy. It can be clarified that the LEDs in sample have the good interfaces and layer periodicities for the strained-layer superlattices and multiple quantum wells. In addition, the optical property in the light output power has been evaluated. As a result, LEDs with a maximum output power of 3.3 mW and a high Saturation operating current of 400 mA have exhibited the good device performance. And, in the section 4.2, the GaN-based LEDs grown by metal-organic chemical vapor

deposition on 4-in. Si(111) substrates have been demonstrated. The structural property has been revealed by the measurement of X-ray diffraction. One of the full widths at half maximum of  $\omega$ -scans of the GaN (0002) reflection is around 630 arcsec. Also, it can be found that the GaN epitaxial quality can be improved by increasing the thickness of n-GaN. The device properties have been evaluated through current-voltage, electroluminescence, and light output power-current measurements. As the n-GaN thickness increases from 1 to 2  $\mu\text{m}$ , the light output powers of the LEDs have enhanced approximately two times under the injection current of 20 mA. Moreover, the maximum values of respective external quantum efficiency are achieved as 0.3 and 0.6%, respectively. Therefore, it can be believed that the high performance of GaN-based LEDs have been realized through this effective approach.

Finally, some points should be taken into account in the future work. Actually, in this study, it is also again proved that the material quality and LEDs performance improvement are limited to GaN epitaxy grown on Si (111). Even though the two approaches have been tried to improve the overall material quality, electrical and optical property in the investigation of epitaxial structure and LEDs performance, there are lots of possible ways for further quality and performance improvement by some combinations with the other methods, such as  $\text{Si}_x\text{N}_{1-x}$  interlayer, etc. Also, there are the other advanced approaches for epitaxial quality improvements, for instance, i) epitaxial lateral overgrowth (ELO), ii) pendo epitaxial overgrowth (PEO), and iii) lateral epitaxial on a patterned substrate (LEPS), etc., which are not yet widely investigated for III-V nitride growth on Si substrate. The above methods are considered to significantly reduce TDD in the epitaxial layers, resulting in a high performance and reliable device lifetime. It can be expected that the advanced growth techniques such as ELO/PEO/LEPS,

and the new approaches, are necessary. While, it must be performed to achieve a commercial-grade high performance GaN-based high brightness LEDs and LD on Si substrate. The author believes that day will be coming by some achievable challenges of lots of researchers, including our group.

## Acknowledgement:

The author would like to appreciate Prof. Takashi Egawa, the director of Research Center of Nano-Device and System, for his constant support to this study, for his valuable directing and encouraging; the author is also grateful to Prof. Shigeo Ohara , Tetuso Soga, Kazuhisa Fujita, Osamu Oda, Associate Prof. Akio Wakejima. and Assitant Prof. Toshiharu Kubo Associate for their constant encouragement and advice during this study. Many thanks are also given to all members and colleagues including previous ones, in particular, Prof. Yang Liu, Baijun Zhang, Hao Jiang, Dr. Jicai Zhang, Zhitao Chen, Lin Lu, Bin Abu Bakar Ahmad Shuhaimi for their kind help and enlighten discussion. Finally, appreciations should be also expressed to the award of doctoral fellowship from the Ministry of Education, Culture, Sports, Science and Technology of Japan (MEXT), for financial support to accomplish this study at Nogoya Institute of Technology.

58